SCIENCE CHINA
Information Sciences

• RESEARCH PAPER •

November 2023, Vol. 66 212203:1–212203:19
https://doi.org/10.1007/s11432-022-3711-1

Structure-free containment control for uncertain underactuated multiple Euler-Lagrange systems

Housheng SU[1], Yali WU[1], Liren ZHANG[1] & Xia CHEN[2*]

[1]*Key Laboratory of Image Processing and Intelligent Control of Education Ministry of China, School of Artificial Intelligence and Automation, Huazhong University of Science and Technology, Wuhan* 430074*, China;*
[2]*State Key Laboratory of Advanced Electromagnetic Engineering and Technology, School of Electrical and Electronic Engineering, Huazhong University of Science and Technology, Wuhan* 430074*, China*

Received 28 May 2022/Revised 27 October 2022/Accepted 16 February 2023/Published online 17 October 2023

Abstract This article studies the problem of structure-free distributed containment control for uncertain underactuated multiple Euler-Lagrange systems (MELSs) considering disturbances by using a layered approach. First, the second layer is the virtual layer constructed artificially for hierarchical control. We move all virtual nodes to the convex hull formed by leaders in the first layer by implementing containment control algorithms on all virtual nodes. Then, the third layer is the following layer, and we propose an adaptive robust tracking controller to ensure that each follower in the third layer tracks the corresponding virtual node in the second layer. So far, the underactuated MELSs can achieve containment control. Furthermore, through the theoretical derivation, sufficient conditions are obtained to achieve the objective of structure-free containment control. Finally, the effectiveness of the proposed stratified structure-free containment control method is verified by a simulation example.

Keywords Euler-Lagrange systems, underactuated system, containment control, adaptive-robust control

Citation Su H S, Wu Y L, Zhang L R, et al. Structure-free containment control for uncertain underactuated multiple Euler-Lagrange systems. Sci China Inf Sci, 2023, 66(11): 212203, https://doi.org/10.1007/s11432-022-3711-1

1 Introduction

Distributed cooperative control refers to a control mode in which a group of agents cooperates to accomplish a common task on the basis of mutual communication and group intelligence. Multiagent systems have considerable advantages in efficiency, flexibility, and reliability, and can be used in various applications (e.g., space interferometers, engagement, and reconnaissance monitoring systems, dangerous goods handling devices, and distributed reconfigurable sensor networks). Distributed cooperative control algorithms can be divided into many types according to control modes and objectives (e.g., consensus [1], flocking [2], and formation control [3]).

The Euler-Lagrange (EL) system has attracted extensive attention since it was developed to model automatic driving, mobile robots, manipulators, and other mechanical systems. Compared with linear systems, the EL system has unique nonlinear characteristics, which make traditional control methods of linear systems no longer applicable but provide an opportunity to design new controllers. In the last decade, the distributed cooperative control of EL systems has become an academic research craze [4–6]. Moreover, in practice, there are many cases where the dimension of control input is less than the degree of freedom of the system, which corresponds to a special type of system called an underactuated system. Underactuated systems have the advantages of lightweight, low energy consumption, and excellent performance, and they are widely used in our work and life (e.g., artificial satellites [7], helicopters [8], and carrier rockets in the oceanographic field; submarines in the ocean field; robot arms in the robotics field; and locomotives and cranes in the transportation field [9], as well as some benchmarking, such as inverted pendulums [10], bat systems, and inertia wheel pendulums). The underactuated characteristics of a system mainly have four causes: the inherent dynamics requirements (e.g., spacecraft, helicopters,

* Corresponding author (email: cxhust@foxmail.com)

and underwater vessels), cost reduction or other purposes (e.g., satellites with two thrusters and flexible linkage robots), driving failure (e.g., surface vessels), and an urge to create complex low-order nonlinear systems artificially (e.g., two-order inverted pendulums and ball-bat systems) to further control high-order underactuated systems. The underactuated system has become a popular control object for the following reasons: underactuated systems widely exist in our lives; in practical engineering, trying to control a system with fewer than the standard number of actuators is meaningful; and the underactuated system is a special type of nonlinear system whose research helps control general nonlinear systems.

Combining the characteristics of EL and underactuated systems, the underactuated EL system is a special system with higher theoretical value and practical engineering value. However, the current mainstream research methods of underactuated EL systems depend on specific physical scenarios [11–15] or require a structurally symmetric inertia matrix [8, 11, 12, 14, 15]. Some researchers solve the uncertainty in the sense of robustness, but they need knowledge of related system terms [11–13] or the disturbance bounds [7], which are often limited. Inspired by the above limitations, structure-free control (i.e., control that is not limited to specific physical scenarios and does not have to meet inertia matrix structural symmetry) for underactuated multiple Euler-Lagrange systems (MELSs) with uncertainties and disturbances becomes a much preferable but challenging choice.

The purpose of containment control is to ultimately drive a group of followers guided by multiple leaders into a convex hull composed of leaders. Many potential applications in the real world have stimulated the study of containment control. For example, when a group of vehicles moves between targets, only some of these vehicles are equipped with the necessary sensors to detect dangerous obstacles. Vehicles equipped with sensors are usually designated as leaders, and other vehicles act as followers. By detecting the locations of dangerous obstacles, leaders can form a dynamic safety zone. If followers stay within the security zone, the team can arrive at the destination safely. In [16], a layered sliding mode control strategy was used to achieve the formation-containment control of multiple underactuated surface vessels (USVs) under-sampling communication conditions. In [17], a predefined performance design approach combined with proper auxiliary variables was used to achieve containment control for uncertain USVs. This control method was simple and did not require any approximators or adaptive components to solve uncertainties. Unfortunately, Refs. [16, 17] were not based on underactuated MELSs.

Motivated by the above literature review, this paper uses a layered approach to study the problem of structure-free distributed containment control for uncertain underactuated MELSs with disturbances. The main contributions are summarized as follows:

(1) Unlike the foregoing three mainstream research methods [11–15], the distributed containment control algorithm adopted in this article is structure-free. In a sense, this attribute extends the processing scope of underactuated EL.

(2) Refs. [18–21] ignored external disturbances and system uncertainties during control, which are well known to exist in practical applications everywhere. Considering external disturbances and system uncertainties helps improve the robustness of a control system. From this viewpoint, the control background of this paper is based on full-dimensional external disturbances and system uncertainties.

(3) Compared with general linear systems [22] or full-actuated EL systems [4–6, 23], the underactuated MELSs discussed in this paper considering external disturbances and system uncertainties perform better in practical applications, which merits further discussion.

Notations. I_p and 1_p denote the $p\times p$ identity matrix and p-dimensional column vector with all ones, respectively. $\|\cdot\|$ denotes the Euclidean norm, and $\lambda_{\min}(\cdot)$ denotes the minimum eigenvalue. $\mathrm{diag}(x_1,\ldots,x_p)$ represents the diagonal matrix. $\mathrm{col}(\xi_1,\ldots,\xi_m)$ denotes the stack column vector. $\mathrm{vec}(A)=[A_1^{\mathrm{T}},\ldots,A_m^{\mathrm{T}}]^{\mathrm{T}}$ represents the heap matrix with $A_i\in\mathcal{R}^{p_i\times q}$.

2 Preliminaries

2.1 Graph theory

The communication network of a multiagent system can be modeled by a directed graph, which is usually expressed as $\mathcal{G}=(\mathcal{V},\mathcal{E},\mathcal{A},\mathcal{L})$ with the node set $\mathcal{V}=\{v_1,v_2,\ldots,v_n\}$, the edge set $\mathcal{E}\subseteq\mathcal{V}\times\mathcal{V}$, the adjacency matrix $\mathcal{A}=[a_{ij}]_{i,j\in\mathcal{V}}\in\mathbb{R}^{n\times n}$, and the Laplacian matrix $\mathcal{L}=[\ell_{ij}]_{i,j\in\mathcal{V}}\in\mathbb{R}^{n\times n}$. An edge from v_i to v_j is denoted by $(v_i,v_j)\in\mathcal{E}$, which means that v_j receives the information from v_i, but not necessarily vice versa. $a_{ji}>0$ if $(v_i,v_j)\in\mathcal{E}$, and v_i is called a neighbor of v_j at this time, otherwise $a_{ji}=0$. Note that

$a_{ii} = 0, i = 1, \ldots, n$. A directed path from v_i to v_j is a sequence of edges expressed as $(v_i, v_k), \ldots, (v_p, v_j)$. Let $\mathcal{N}_j$ denote the set of neighbors of v_j. The Laplacian matrix is defined to satisfy $\ell_{ij} = -a_{ij}, i \neq j$, and $\ell_{ii} = \sum_{j=1, j\neq i}^{n} a_{ij}$ [24].

In this article, we consider a directed topology $\bar{\mathcal{G}}_{\mathcal{A}}$ with N_r leaders and N_f followers numbered as $1, \ldots, N_r, N_r + 1, \ldots, N_r + N_f$ successively. Let $\mathcal{G}_{\mathcal{A}}$ denote the subgraph consisting of N_f followers. Let $\bar{\mathcal{A}}$, $\mathcal{A}$, $\bar{\mathcal{L}}$, $\mathcal{L}$ denote the adjacency matrix and Laplacian matrix of $\bar{\mathcal{G}}_{\mathcal{A}}$ and $\mathcal{G}_{\mathcal{A}}$, respectively. Besides, as for $\bar{\mathcal{G}}_{\mathcal{A}}$, we use ω_i^k to indicate the direct connectivity of the i-th follower to the k-th leader and let Ω_k be $\mathrm{diag}\{\omega_{N_r+1}^k, \ldots, \omega_{N_r+N_f}^k\}$.

2.2 Problem formulation

The leaders have dynamics as follows:

$$\dot{\eta}_i = S\eta_i, \tag{1a}$$

$$q_i = C\eta_i,\ i \in \mathcal{R}, \tag{1b}$$

where $\mathcal{R} = \{1, \ldots, N_r\}$ denotes the leader set, and $q_i \in \mathbb{R}^n, i \in \mathcal{R}$ is the generalized position of the i-th leader, $\eta_i \in \mathbb{R}^p$ is the internal state, and $S \in \mathbb{R}^{p\times p}$ and $C \in \mathbb{R}^{n\times p}$ are constant matrices. The leaders satisfy the following assumptions.

Assumption 1. $q_i(t), \dot{q}_i(t), \ddot{q}_i(t)$, $i \in \mathcal{R}$ exist and are bounded.

Assumption 2. All the eigenvalues of S are semi-simple with zero real parts.

Remark 1. Under Assumption 2, the leader system (1a) can generate a large class of time-varying signals such as the step signal of arbitrary magnitude, the sinusoidal signal of arbitrary amplitude, frequency, and phase angle, and any signal which is a combination of a finite number of step signals and sinusoidal signals. In particular, let $\eta_i(t) = [\eta_{i1}(t), \ldots, \eta_{ip}(t)]^{\mathrm{T}}, i \in \mathcal{R}$. Then, $\eta_{ij}(t), j = 1, \ldots, p$ can take the following form:

$$\eta_{ij}(t) = a_i(t) + \sum_{i=1}^{n_i}(a_{ij}\sin\omega_{ij}t + \phi_{ij}),$$

where n_i is an arbitrary positive integer, $a_i(t)$ is an unknown step magnitude, a_{ij}, ω_{ij}, and ϕ_{ij} are unknown amplitudes, frequencies, and phase angles, respectively. Then $q_i(t), \dot{q}_i(t), \ddot{q}_i(t), i \in \mathcal{R}$ exist and are bounded.

Remark 2. In this paper, we focus on the more realistic case in which η_i, S, C can only be obtained by those followers who can communicate with the leaders. In other words, only part of the followers need to know the dynamic information of the leaders.

Definition 1. The convex hull for $\mathcal{Q}_{\mathcal{R}} = \{q_1, \ldots, q_{N_r}\}$ can be represented as $\mathrm{Co}(\mathcal{Q}_{\mathcal{R}}) = \{\sum_{i=1}^{N_r} a_i q_i | a_i \geqslant 0, \sum_{i=1}^{N_r} a_i = 1\}$.

The followers conform to the underactuated Euler-Lagrange model:

$$M_i(q_i)\ddot{q}_i + V_{m_i}(q_i, \dot{q}_i)\dot{q}_i + G_i(q_i) + F_i(\dot{q}_i) + \varpi_i(t) = [\tau_i^{\mathrm{T}}\ 0^{\mathrm{T}}]^{\mathrm{T}},\ i \in \mathcal{F}, \tag{2}$$

where $\mathcal{F} = \{N_r + 1, \ldots, N_r + N_f\}$ denotes the follower set, and $q_i(t), \dot{q}_i(t), \ddot{q}_i(t) \in \mathbb{R}^n, i \in \mathcal{F}$ are the position, velocity, and acceleration of the i-th follower respectively. $\tau_i \in \mathbb{R}^m$ denotes the control force where $n - m < m < n$. $M_i(q_i) \in \mathbb{R}^{n\times n}$ represents the inertia matrix, $V_{m_i}(q_i, \dot{q}_i) \in \mathbb{R}^{n\times n}$ denotes the centripetal-Coriolis matrix, $G_i(q_i) \in \mathbb{R}^n$ denotes the gravity vector, $F_i(\dot{q}_i) \in \mathbb{R}^n$ is the friction vector, and $\varpi_i(t) \in \mathbb{R}^n$ refers to the external disturbance.

Some propositions and assumptions about the underactuated EL system (2) are listed as follows [25].

Proposition 1. $\|V_{m_i}(q_i, \dot{q}_i)\| \leqslant \bar{v}_{m_i}\|\dot{q}_i\|$, $\|G_i(q_i)\| \leqslant \bar{g}_i$, $\|F_i(\dot{q}_i)\| \leqslant \bar{f}_i\|\dot{q}_i\|$, $\|\varpi_i(q_i)\| \leqslant \bar{\varpi}_i$, where $\bar{v}_{m_i}, \bar{g}_i, \bar{f}_i, \bar{\varpi}_i \in \mathbb{R}^+$. Moreover, V_{m_i}, G_i, F_i, ϖ_i, $\bar{v}_{m_i}$, $\bar{g}_i$, $\bar{f}_i$, $\bar{\varpi}_i$ are unknown.

Proposition 2. $M_i(q_i)$ is a symmetric uniformly positive definite matrix, and has the following characteristic:

$$0 < \mu_i^1 I_n \leqslant M_i(q_i) \leqslant \mu_i^2 I_n,$$

where $\mu_i^1, \mu_i^2 \in \mathbb{R}^+$.

Assumption 3. Decompose M_i as $M_i = \hat{M}_i + \breve{M}_i$, where $\hat{M}_i$ is the nominal value of M_i and $\breve{M}_i$ is the perturbation value of M_i. Only $\hat{M}_i$ and the upper bound of $\breve{M}_i$ are assumed to be available.

Assumption 4. $q_i, \dot{q}_i, i \in \mathcal{F}$ are measurable.

The entire discussion is based on the following topology assumption.

Assumption 5. For each of the followers, there exists at least one leader that has a directed path to the follower.

Definition 2. The multiagent system (1a)–(2) is judged to have achieved containment if

$$\lim_{t\to\infty} \mathcal{Q}_{\mathcal{F}} \to \mathrm{Co}(\mathcal{Q}_{\mathcal{R}}),$$

in which $\mathcal{Q}_{\mathcal{F}} = \{q_{N_r+1}, \ldots, q_{N_r+N_f}\}$.

3 Observer design

The first step of hierarchical control is to construct the virtual layer artificially, and design the following distributed containment observer to make all virtual nodes converge to the convex hull composed of leaders in the leader layer.

$$\dot{S}_i = k_1 \left(\sum_{j=N_r+1}^{N_r+N_f} a_{ij}(S_j - S_i) + \sum_{k=1}^{N_r} \omega_i^k (S_k - S_i) \right), \tag{3a}$$

$$\dot{C}_i = k_2 \left(\sum_{j=N_r+1}^{N_r+N_f} a_{ij}(C_j - C_i) + \sum_{k=1}^{N_r} \omega_i^k (C_k - C_i) \right), \tag{3b}$$

$$\dot{\xi}_i = S_i \xi_i + k_3 \left(\sum_{j=N_r+1}^{N_r+N_f} a_{ij}(\xi_j - \xi_i) + \sum_{k=1}^{N_r} \omega_i^k (\xi_k - \xi_i) \right), \tag{3c}$$

where $S_i, C_i, i \in \mathcal{F}$ are the estimated values of S, C, respectively, and $S_k = S, C_k = C, k = 1, \ldots, N_r$. $\xi_i, i \in \mathcal{F}$ can be viewed as the estimated value of the convex hull $\mathrm{Co}(\eta_k), k \in \mathcal{R}$, and $\xi_k = \eta_k, k = 1, \ldots, N_r$.

Remark 3. Notice that Eqs. (3a) and (3b) can be rewritten in a uniform form as $\dot{T}_i = \bar{k} \sum_{j=1}^{N_r+N_f} \bar{a}_{ij}(T_j - T_i), \bar{k} > 0$, where $T_i \in \mathbb{R}^{a\times b}, i \in \mathcal{R} \cup \mathcal{F}$ represents $S_i, C_i, i \in \mathcal{R} \cup \mathcal{F}$. $\bar{a}_{ij}$ is the element of the adjacency matrix $\bar{\mathcal{A}} \in \mathbb{R}^{(N_r+N_f)\times(N_r+N_f)}$. In the following proof, we will uniformly adopt this form for (3a) and (3b).

Before we begin the proof of (3a)–(3c), we need to introduce the following lemma [26,27].

Lemma 1. Let $Z_k = \frac{\mathcal{L}}{N_r} + \Omega_k, k \in \mathcal{R}$. Under Assumption 5, Z_k is a positive definite nonsingular $\mathcal{M}$-matrix. Let $Z = \Sigma_{k=1}^{N_r} Z_k$. Then, there exists a diagonal matrix $\Theta = \mathrm{diag}\{\theta_1, \theta_2, \ldots, \theta_{N_f}\}$ with $\theta_i > 0$ and $\sum_{i=1}^{N_f} \theta_i = 1$ for any $i = 1, 2, \ldots, N_f$, such that the symmetric matrix

$$\widehat{Z} = \Theta Z + Z^{\mathrm{T}} \Theta$$

is positive definite.

Theorem 1. Using (3a)–(3c), if k_1, k_2, k_3 are large enough, then the virtual layer can achieve containment for arbitrary initial conditions under Assumption 5.

Proof. Since $S_k = S, C_k = C, k \in \mathcal{R}$, when we focus on the variable T_k (i.e., S_k, C_k), all leaders can be naturally considered the same agent, which we will call agent 0 next, thus $T_0(t) \equiv T$ (i.e., S, C). Next, considering the new network topology $\bar{\mathcal{G}}_{\mathcal{B}}$ which contains N_f followers and agent 0, we have

$$\dot{T}_i = \bar{k} \sum_{j=0\cup\mathcal{F}} \bar{b}_{ij}(T_j - T_i), \ i \in \mathcal{F}, \tag{4}$$

where $\bar{b}_{ij}$ is the element of the new adjacency matrix $\bar{\mathcal{B}}$ which corresponds to the new network topology $\bar{\mathcal{G}}_{\mathcal{B}}$. According to Assumption 5, the new subgraph $\mathcal{G}_{\bar{B}}$ is a spanning tree and the agent 0 is the root.

Let error variables $\tilde{T}_i = T_i - T_0$, and $\tilde{T} = \mathrm{col}(\tilde{T}_{N_r+1}, \ldots, \tilde{T}_{N_r+N_f})$; then we have

$$\mathrm{vec}(\dot{\tilde{T}}) = -\bar{k}(I_b \otimes \bar{H}_B \otimes I_a)\mathrm{vec}(\tilde{T}), \tag{5}$$

where $\bar{H}_B = \mathcal{L}_{\mathcal{B}} + \mathrm{diag}\{\bar{b}_{(N_r+1)0}, \ldots, \bar{b}_{(N_r+N_f)0}\}$, and $\mathcal{L}_{\mathcal{B}}$ is the Laplacian matrix of $\mathcal{G}_{\mathcal{B}}$.

By Corollary 1 of [28], when $\bar{k}$ is sufficiently large, Eq. (5) can be concluded to be exponentially stable, which implies that $T_i \to T_0$ as $t \to \infty$. That is, $S_i \to S$, $C_i \to C$ as $t \to \infty$.

Next we need to prove that $\xi = \mathrm{col}(\xi_{Nr+1}, \ldots, \xi_{Nr+N_f})$ converges to the overall convex hull $\mathrm{Co}(\eta) = \sum_{k=1}^{N_r} \left\{ \left((\sum_{l=1}^{N_r} Z_l)^{-1} Z_k 1_{N_f} \right) \otimes \eta_k \right\}$ by (3c).

Step 1. To prove that $\mathrm{Co}(\eta) = \sum_{k=1}^{N_r} \left\{ \left[(\sum_{l=1}^{N_r} Z_l)^{-1} Z_k 1_{N_f} \right] \otimes \eta_k \right\}$ is the overall convex hull of $\eta_k, k \in \mathcal{R}$.

According to Definition 1, we need to achieve this by verifying the following two conditions.

(i) The sum of the combined coefficients of the convex hull is equal to 1. In fact,

$$\sum_{k=1}^{N_r} \left(\left(\sum_{l=1}^{N_r} Z_l \right)^{-1} Z_k 1_{N_f} \right) = \left(\sum_{l=1}^{N_r} Z_l \right)^{-1} \left(\sum_{k=1}^{N_r} Z_k 1_{N_f} \right) = 1_{N_f}. \tag{6}$$

(ii) Every combined coefficient of the convex hull is nonnegative. Let $(\sum_{l=1}^{N_r} Z_l)^{-1} = [c_{ij}]$ and $(\sum_{l=1}^{N_r} Z_l)^{-1} Z_k 1_{N_f} = \mathrm{col}(d_{ki})$. Thus, we have

$$d_{ki} = \sum_{j=N_r+1}^{N_r+N_f} c_{ij} w_j^k + \frac{1}{N_r} \sum_{j=N_r+1}^{N_r+N_f} c_{ij} \left(\sum_{l=N_r+1}^{N_r+N_f} l_{jl} \right), \ k \in \mathcal{R}. \tag{7}$$

Because the sum of the elements in each row of the Laplacian matrix is 0, Eq. (7) can be simplified as

$$d_{ki} = \sum_{j=N_r+1}^{N_r+N_f} c_{ij} w_j^k, \ k \in \mathcal{R}. \tag{8}$$

Based on Lemma 1, we can infer that $(\sum_{l=1}^{N_r} Z_l)^{-1}$ exists and is nonnegative, which implies that $c_{ij}, i, j \in \mathcal{F}$ is nonnegative. Meanwhile, note that $w_j^k, j \in \mathcal{F}, k \in \mathcal{R}$ is nonnegative. From (8), we can conclude that every combined coefficient $d_{ki}, i \in \mathcal{F}, k \in \mathcal{R}$ is nonnegative.

Step 2. To prove that the observer (3c) guarantees to converge to the overall convex hull $\mathrm{Co}(\eta)$.

For the sake of subsequent proof, rewrite $\mathrm{Co}(\eta)$ as $\mathrm{Co}(\eta) = (\sum_{l=1}^{N_r} \bar{Z}_l)^{-1} \sum_{k=1}^{N_r} \bar{Z}_k \bar{\eta}_k$, in which $\bar{Z}_k = Z_k \otimes I_p, \bar{\eta}_k = 1_{N_f} \otimes \eta_k$. Let $\tilde{\xi} = \xi - (\sum_{l=1}^{N_r} \bar{Z}_l)^{-1} \sum_{k=1}^{N_r} \bar{Z}_k \bar{\eta}_k$. From (1a), we have

$$\dot{\tilde{\xi}} = \dot{\xi} - \sum_{k=1}^{N_r} \left[\left(\sum_{l=1}^{N_r} \bar{Z}_l \right)^{-1} \bar{Z}_k \bar{S} \bar{\eta}_k \right], \tag{9}$$

where $\bar{S} = I_{N_f} \otimes S$.

And from (3c), Eq. (9) can derive that

$$\begin{aligned} \dot{\tilde{\xi}} &= \left(\bar{S} - k_3 \sum_{k=1}^{N_r} \bar{Z}_k \right) \xi + k_3 \sum_{k=1}^{N_r} \bar{Z}_k \bar{\eta}_k - \bar{S} \left(\sum_{l=1}^{N_r} \bar{Z}_l \right)^{-1} \sum_{k=1}^{N_r} \bar{Z}_k \bar{\eta}_k \\ &= \left(\bar{S} - k_3 \sum_{k=1}^{N_r} \bar{Z}_k \right) \left(\xi - \left(\sum_{l=1}^{N_r} \bar{Z}_l \right)^{-1} \sum_{k=1}^{N_r} \bar{Z}_k \bar{\eta}_k \right) \\ &= \left(\bar{S} - k_3 \sum_{k=1}^{N_r} \bar{Z}_k \right) \tilde{\xi}. \end{aligned} \tag{10}$$

Define a Lyapunov function $V(\tilde{\xi}(t)) = \tilde{\xi}^{\mathrm{T}} (\Theta \otimes I_p) \tilde{\xi}$. Then, we have $\dot{V}(\tilde{\xi}(t)) = \tilde{\xi}^{\mathrm{T}} [2(\Theta \otimes I_p)\bar{S} - k_3((\Theta Z + Z^{\mathrm{T}}\Theta) \otimes I_p)] \tilde{\xi} \leqslant -[k_3 \lambda_{\min}(\widehat{Z}) - 2\|\bar{S}\|] \tilde{\xi}^{\mathrm{T}} \tilde{\xi}$. According to Lemma 1, $\lambda_{\min}(\widehat{Z})$ is positive. Hence, we can ensure that $-[k_3 \lambda_{\min}(\widehat{Z}) - 2\|\bar{S}\|]$ is negative, provided we select k_3 large enough. In this way, $\dot{V}(\tilde{\xi}(t)) = -[k_3 \lambda_{\min}(\widehat{Z}) - 2\|\bar{S}\|] V(\tilde{\xi}(t))$, resulting in $\lim_{t \to \infty} \tilde{\xi} = 0$. By Steps 1 and 2, we can give a conclusion that Eq. (3c) can perform a function to observe the convex hull $\mathrm{Co}(\eta)$.

Since $\lim_{t\to\infty} C_i = C$, $i \in \mathcal{F}$, let $\zeta = \mathrm{diag}(C_{N_r+1}, \ldots, C_{N_r+N_f})\xi$. Based on the equivalent substitution theorem, we have

$$\lim_{t\to\infty} \Big(\zeta - \mathrm{col}(q_1, \ldots, q_{N_r})\Big) = \lim_{t\to\infty} \mathrm{diag}(C, \ldots, C)\tilde{\xi} = 0, \tag{11}$$

and

$$\lim_{t\to\infty} \Big(\dot{\zeta} - \mathrm{col}(\dot{q_1}, \ldots, \dot{q}_{N_r})\Big) = \lim_{t\to\infty} \mathrm{diag}(\dot{C}, \ldots, \dot{C})\dot{\tilde{\xi}} = 0, \tag{12}$$

which implies Eqs. (3a)–(3c) can perform a function to observe the convex hull $\mathrm{Co}(\mathcal{Q}_{\mathcal{R}})$.

4 Control design

4.1 Control objective

The control objective is to achieve structure-free containment control for underactuated MELSs under the condition of uncertainties and disturbances.

The second step of hierarchical control is to design an adaptive robust tracking controller to make each follower in the following layer track the corresponding virtual node in the virtual layer.

For the convenience of subsequent control, rewrite (2) by separating actuated states and non-actuated states as

$$M_i(q_i)\ddot{q}_i + Y_i(q_i, \dot{q}_i) + \varpi_i(t) = [\tau_i^{\mathrm{T}}\ 0^{\mathrm{T}}]^{\mathrm{T}},\ i \in \mathcal{F}, \tag{13}$$

where $q_i = [q_{i_a}^{\mathrm{T}}\ q_{i_u}^{\mathrm{T}}]^{\mathrm{T}}$. $q_{i_a} \in \mathbb{R}^m$ and $q_{i_u} \in \mathbb{R}^{n-m}$ are actuated states and non-actuated states, respectively. In (13), the system matrices and disturbance can be partitioned as follows:

$$M_i \triangleq \begin{bmatrix} M_{i_{aa}} & M_{i_{au}} \\ M_{i_{au}}^{\mathrm{T}} & M_{i_{uu}} \end{bmatrix}, \tag{14a}$$

$$Y_i \triangleq V_{m_i}(q_i, \dot{q}_i)\dot{q}_i + G_i(q_i) + F_i(\dot{q}_i) = [Y_{i_a}^{\mathrm{T}}\ Y_{i_u}^{\mathrm{T}}]^{\mathrm{T}}, \tag{14b}$$

$$\varpi_i \triangleq [\varpi_{i_a}^{\mathrm{T}}\ \varpi_{i_u}^{\mathrm{T}}]^{\mathrm{T}}, \tag{14c}$$

where $M_{i_{aa}} \in \mathbb{R}^{m\times m}$, $M_{i_{au}} \in \mathbb{R}^{m\times(n-m)}$, $M_{i_{uu}} \in \mathbb{R}^{(n-m)\times(n-m)}$, $Y_{i_a} \in \mathbb{R}^m$, $Y_{i_u} \in \mathbb{R}^{(n-m)}$, $\varpi_{i_a} \in \mathbb{R}^m$, and $\varpi_{i_u} \in \mathbb{R}^{(n-m)}$.

According to (13)–(14c), the original underactuated EL dynamics (2) can be disassembled into two coupled subsystems as

$$\ddot{q}_{i_a} = M_{i_a}^{-1}\tau_i + y_{i_a}, \tag{15a}$$

$$\ddot{q}_{i_u} = -M_{i_{uu}}^{-1}M_{i_{au}}^{\mathrm{T}}\ddot{q}_{i_a} + y_{i_u}, \tag{15b}$$

where $M_{i_a} \triangleq M_{i_{aa}} - M_{i_{au}}M_{i_{uu}}^{-1}M_{i_{au}}^{\mathrm{T}}$, $y_{i_a} \triangleq -M_{i_a}^{-1}(Y_{i_a} + \varpi_{i_a} + M_{i_{au}}y_{i_u})$, $y_{i_u} \triangleq -M_{i_{uu}}^{-1}(Y_{i_u} + \varpi_{i_u})$.

Assumption 6. The block $M_{i_{au}}$ is full rank.

Remark 4. Assumption 6 avoids morbid conditions such as $M_{i_{au}}$ being zero, which would lead to the uncontrollability of the non-actuated subsystem (15b).

4.2 Open-loop error system

Redefine $\zeta_i = [\zeta_{i_a}^{\mathrm{T}}\ \zeta_{i_u}^{\mathrm{T}}]^{\mathrm{T}}, i \in \mathcal{F}$. Construct tracking error variables of actuated and non-actuated states as well as the compound error variable for each follower, respectively, as follows:

$$e_{i_a} = q_{i_a} - \zeta_{i_a}, \tag{16a}$$

$$e_{i_u} = q_{i_u} - \zeta_{i_u}, \tag{16b}$$

$$r_i = K_a\dot{e}_{i_a} + \Theta_a e_{i_a} + K_u\dot{e}_{i_u} + \Theta_u e_{i_u}, \tag{16c}$$

where $K_a, \Theta_a \in \mathbb{R}^{m\times m} > 0$ satisfying $K_a^{-1}\Theta_a > 0$. $K_u, \Theta_u \in \mathbb{R}^{m\times(n-m)}$ are of full rank.

By (15a) and (15b), the open-loop error dynamic of r_i yields

$$\dot{r}_i = K_a\ddot{e}_{i_a} + \Theta_a\dot{e}_{i_a} + K_u\ddot{e}_{i_u} + \Theta_u\dot{e}_{i_u}$$

$$
\begin{aligned}
=&\underbrace{(K_a - K_u M_{i_{uu}}^{-1} M_{i_{au}}^{\mathrm{T}}) M_{i_a}^{-1}}_{d_i} \tau_i \\
&+ \underbrace{(K_a - K_u M_{i_{uu}}^{-1} M_{i_{au}}^{\mathrm{T}}) y_{i_a} + K_a y_{i_u} - K_a \ddot{\zeta}_{i_a} - K_u \ddot{\zeta}_{i_u}}_{\Phi_i} \\
&+ \underbrace{\Theta_a \dot{e}_{i_a} + \Theta_u \dot{e}_{i_u}}_{\Xi_i} \\
=&d_i \tau_i + \Phi_i + \Xi_i. \qquad (17)
\end{aligned}
$$

4.3 Closed-loop error system

Based on (17), the adaptive robust controller can be designed as follows:

$$\tau_i = \hat{d}_i(-\Lambda r_i - \Xi_i - \breve{\tau}_i),\ i \in \mathcal{F}, \tag{18a}$$

$$\breve{\tau}_i = \begin{cases} u_i \frac{r_i}{\|r_i\|}, & \|r_i\| \geqslant r^{(0)}, \\ u_i \frac{r_i}{r^{(0)}}, & \|r_i\| < r^{(0)}, \end{cases} \tag{18b}$$

where $\Lambda \in \mathbb{R}^{m\times m} > 0$. The adaptive gain coefficient u_i will be designed later, and $r^{(0)}$ is a small positive scalar. $\hat{d}_i$ can be regarded as the nominal value of d_i, which has the following proposition.

Proposition 3. $\|d_i \hat{d}_i^{-1} - I_m\| \leqslant H_i < 1$, where H_i is a known positive number.

Remark 5. Proposition 3 is derived from Assumption A3 in [29].

Using (18a) and (18b), the closed-loop error dynamics of r_i can be attained,

$$\dot{r}_i = -\Lambda r_i - \breve{\tau}_i + \underbrace{\Phi_i - (d_i \hat{d}_i^{-1} - I_m)(\Lambda r_i + \Xi_i)}_{\bar{\Phi}_i} - (d_i \hat{d}_i^{-1} - I_m)\breve{\tau}_i. \tag{19}$$

By Propositions 1 and 2, we can infer

$$\|Y_i\| \leqslant \|V_{m_i}\| \|\dot{q}_i\| + \|G_i\| + \|F_i\| \leqslant \bar{v}_{m_i} \|\dot{q}_i\|^2 + \bar{f}_i \|\dot{q}_i\| + \bar{g}_i. \tag{20}$$

Define $\bar{e}_i \triangleq [e_i^{\mathrm{T}}\ \dot{e}_i^{\mathrm{T}}]^{\mathrm{T}} = [e_{i_a}^{\mathrm{T}}\ e_{i_u}^{\mathrm{T}}\ \dot{e}_{i_a}^{\mathrm{T}}\ \dot{e}_{i_u}^{\mathrm{T}}]^{\mathrm{T}}$. Note that $\|e_i\| \leqslant \|\bar{e}_i\|$ and $\|\dot{e}_i\| \leqslant \|\bar{e}_i\|$. Since $e_i \triangleq q_i - \zeta_i$, that is, $q_i = e_i + \zeta_i$, we get

$$\|q_i\| \leqslant \|e_i\| + \|\zeta_i\| \leqslant \|\bar{e}_i\| + \|\zeta_i\|, \tag{21a}$$

$$\|\dot{q}_i\| \leqslant \|\dot{e}_i\| + \left\|\dot{\zeta}_i\right\| \leqslant \|\bar{e}_i\| + \left\|\dot{\zeta}_i\right\|. \tag{21b}$$

Squaring both sides of (21b), we can obtain

$$\|\dot{q}_i\|^2 \leqslant \|\bar{e}_i\|^2 + \left\|\dot{\zeta}_i\right\|^2 + 2\|\bar{e}_i\| \left\|\dot{\zeta}_i\right\|. \tag{22}$$

By (21b) and (22), Eq. (20) can be further scaled up to

$$\|Y_i\| \leqslant \bar{v}_{m_i}\left(\|\bar{e}_i\|^2 + \left\|\dot{\zeta}_i\right\|^2 + 2\|\bar{e}_i\| \left\|\dot{\zeta}_i\right\|\right) + \bar{f}_i\left(\|\bar{e}_i\| + \left\|\dot{\zeta}_i\right\|\right) + \bar{g}_i. \tag{23}$$

Then,

$$
\begin{aligned}
\left\|\bar{\Phi}_i\right\| &= \left\|\Phi_i - \left(d_i \hat{d}_i^{-1} - I_m\right)(\Lambda r_i + \Xi_i)\right\| \\
&\leqslant \|\Phi_i\| + H_i(\|\Lambda\| \|r_i\| + \|\Xi_i\|) \\
&\leqslant \vartheta_{2,i}^* \|\bar{e}_i\|^2 + \vartheta_{1,i}^* \|\bar{e}_i\| + \vartheta_{0,i}^*, \qquad (24)
\end{aligned}
$$

with

$$\vartheta_{2,i}^* \triangleq a_{1,i} \bar{v}_{m_i}, \tag{25a}$$

$$\vartheta_{1,i}^{*} \triangleq H_i\Big(\|\Lambda\| \left(\|K_a\| + \|\Theta_a\| + \|K_u\| + \|\Theta_u\|\right) + \|\Theta_a\| + \|\Theta_u\| \Big) + a_{1,i}\left(2\bar{v}_{m_i}\left\|\dot{\zeta}_i\right\| + \bar{f}_i\right), \tag{25b}$$

$$\vartheta_{0,i}^{*} \triangleq a_{1,i}\left(\bar{v}_{m_i}\left\|\dot{\zeta}_i\right\|^2 + \bar{f}_i\|\zeta_i\| + \bar{g}_i + \bar{\varpi}_i\right) + \|K_a\|\left\|\ddot{\zeta}_{i_a}\right\| + \|K_u\|\left\|\ddot{\zeta}_{i_u}\right\|, \tag{25c}$$

$$a_{1,i} \triangleq \left\|K_a - K_u M_{i_{uu}}^{-1} M_{i_{au}}^{\mathrm{T}}\right\| \left\|M_{i_a}^{-1}\right\| \left(1 + \left\|M_{i_{au}} M_{i_{uu}}^{-1}\right\|\right) + \|K_u\|\left\|M_{i_{uu}}^{-1}\right\|. \tag{25d}$$

Meanwhile, from (15a) and (15b), the open-loop dynamics of e_{i_u} yields

$$\begin{aligned}\ddot{e}_{i_u} &= \ddot{q}_{i_u} - \ddot{\zeta}_{i_u} \\ &= -M_{i_{uu}}^{-1} M_{i_{au}}^{\mathrm{T}} \ddot{q}_{i_a} + y_{i_u} - \ddot{\zeta}_{i_u} \\ &= -M_{i_{uu}}^{-1} M_{i_{au}}^{\mathrm{T}} (M_{i_a}^{-1}\tau_i + y_{i_a}) + y_{i_u} - \ddot{\zeta}_{i_u}.\end{aligned} \tag{26}$$

By (18a) and (18b), letting $e_{i_u}^{(0)} \triangleq e_{i_u}$ and $e_{i_u}^{(1)} \triangleq \dot{e}_{i_u}$, the closed-loop dynamics of e_{i_u} can be represented as

$$\dot{e}_{i_u}^{(0)} = e_{i_u}^{(1)}, \tag{27a}$$

$$\begin{aligned}\dot{e}_{i_u}^{1} &= -\underbrace{M_{i_{uu}}^{-1} M_{i_{au}}^{\mathrm{T}} M_{i_a}^{-1} \hat{d}_i^{-1}}_{g_i} \underbrace{(-\Lambda r_i - \Xi_i - \breve{\tau}_i)}_{x_i} - \underbrace{(M_{i_{uu}}^{-1} M_{i_{au}}^{\mathrm{T}} y_{i_a} - y_{i_u})}_{\varphi_{1_i}} - \ddot{\zeta}_{i_u} \\ &= -g_i x_i - \varphi_{1_i} - \ddot{\zeta}_{i_u}.\end{aligned} \tag{27b}$$

Since $n - m \leqslant m < n$, by designing a full-rank matrix K which satisfies:

$$\Upsilon_1 \triangleq K\Lambda\Theta_u > 0,\ \Upsilon_2 \triangleq K\Lambda K_u > 0, \tag{28}$$

and adding and subtracting Kx_i to (27b), we get

$$\dot{e}_{i_u}^{(0)} = e_{i_u}^{(1)}, \tag{29a}$$

$$\begin{aligned}\dot{e}_{i_u}^{(1)} &= \underbrace{g_i\Xi_i + (K + g_i)\Lambda r_i - \varphi_{1_i} - K\Lambda(K_a\dot{e}_{i_a} + \Theta_a e_{i_a}) - \ddot{\zeta}_{i_u}}_{\varphi_{2_i}} \\ &\quad - \Upsilon_1 e_{i_u}^{(0)} - \Upsilon_2 e_{i_u}^{(1)} + g_i\breve{\tau}_i \\ &= -\Upsilon_1 e_{i_u}^{(0)} - \Upsilon_2 e_{i_u}^{(1)} + g_i\breve{\tau}_i + \varphi_{2_i}.\end{aligned} \tag{29b}$$

Here, define $E_i \triangleq [e_{i_u}^{(0)^{\mathrm{T}}}\ e_{i_u}^{(1)^{\mathrm{T}}}]^{\mathrm{T}}$; then Eqs. (29a) and (29b) can be combined into the matrix form:

$$\dot{E}_i = AE_i + B(g_i\breve{\tau}_i + \varphi_{2_i}), \tag{30}$$

where $A \triangleq \left[\begin{smallmatrix} 0 & I_{(n-m)} \\ -\Upsilon_1 & -\Upsilon_2 \end{smallmatrix}\right]$ is Hurwitz and $B \triangleq [0\ I_{(n-m)}]^{\mathrm{T}}$.

Based on Propositions 1 and 2, it can be concluded that

$$\|\varphi_{2_i}\|\|PB\| \leqslant \vartheta_{2,i}^{**}\|\bar{e}_i\|^2 + \vartheta_{1,i}^{**}\|\bar{e}_i\| + \vartheta_{0,i}^{**}, \tag{31}$$

with

$$\vartheta_{2,i}^{**} \triangleq a_{3,i}\bar{v}_{m_i}\|PB\|, \tag{32a}$$

$$\vartheta_{1,i}^{**} \triangleq \Big(a_{2,i}\|\Lambda\|\left(\|K_a\| + \|\Theta_a\| + \|K_u\| + \|\Theta_u\|\right) + \|K\Lambda\|\left(\|K_u\| + \|\Theta_u\|\right) + \bar{f}_i a_{3,i}\Big)\|PB\|, \tag{32b}$$

$$\vartheta_{0,i}^{**} \triangleq \Big(a_{2,i}(\|\Theta_a\| + \|\Theta_u\|) + (\bar{g}_i + \bar{\varpi}_i)a_{3,i} + \Big\|\ddot{\zeta}_{i_u}\Big\|\Big) \|PB\|, \tag{32c}$$

$$a_{2,i} \triangleq \Big\|M_{i_{uu}}^{-1} M_{i_{au}}^{\mathrm{T}} M_{i_a}^{-1} \hat{M}_{i_a} (K_a - K_u \hat{M}_{i_{uu}}^{-1} \hat{M}_{i_{au}}^{\mathrm{T}})^{-1}\Big\|, \tag{32d}$$

$$a_{3,i} \triangleq \big\|M_{i_{uu}}^{-1} M_{i_{au}}^{\mathrm{T}} M_{i_a}^{-1}\big\| \left(1 + \big\|M_{i_{au}} M_{i_{uu}}^{-1}\big\|\right) + \big\|M_{i_{uu}}^{-1}\big\|, \tag{32e}$$

where P is the solution to the Lyapunov equation $A^{\mathrm{T}}P + PA = -Q$ in which Q is a user-defined positive definite matrix. $\bar{\Phi}_i$ and φ_{2_i} can be regarded as the overall uncertainty of (19) and (30), respectively.

Now, design the adaptive gain coefficient u_i as

$$u_i = \frac{\hat{\vartheta}_{0,i} + \hat{\vartheta}_{1,i} \|\bar{e}_i\| + \hat{\vartheta}_{2,i} \|\bar{e}_i\|^2 + \pi_i}{1 - H_i}, \tag{33a}$$

$$\dot{\hat{\vartheta}}_{k,i} = \bar{b}_{k,i}(\|r_i\| + \|E_i\|) \|\bar{e}_i\|^k - \bar{c}_{k,i}\hat{\vartheta}_{k,i}k_{4,i} \|E_i\| \|\bar{e}_i\|^k, \tag{33b}$$

$$\begin{aligned}\dot{\pi}_i = &-\pi_i\{k_{5,i} + k_{6,i}(\|\bar{e}_i\|^5 - \|\bar{e}_i\|^4) + k_{7,i}(\|E_i\| + \|\bar{e}_i\|)\} \\ &+ k_{5,i}(\|r_i\| + \|E_i\| + k_{8,i}),\ i \in \mathcal{F},\end{aligned} \tag{33c}$$

with

$$\hat{\vartheta}_{k,i}(0) > 0, \tag{34a}$$

$$\pi_i(0) > k_{8,i}, \tag{34b}$$

$$\bar{b}_{k,i}, \bar{c}_{k,i}, k_{4,i}, k_{5,i}, k_{6,i}, k_{7,i}, k_{8,i} > 0, \tag{34c}$$

$$k_{7,i} \geqslant k_{6,i}, \tag{34d}$$

$$k_{4,i} > 1 + \frac{\bar{P}_i}{1 - H_i}, \tag{34e}$$

where the subscript and superscript $k = 0, 1, 2$, $\bar{P}_i$ is the upper bound of $\|PBg_i\|$, and $\hat{\vartheta}_{k,i}$ acts as the estimate of $\bar{\vartheta}_{k,i} \triangleq \sup\big\|\max\{\vartheta_{k,i}^*, \vartheta_{k,i}^{**}\}\big\|$.

4.4 Stability analysis

Theorem 2. Supposing Assumptions 1–6 and Propositions 1–3 hold, the adaptive robust tracking controller (18a)–(18b), (33a)–(33c) with the containment observer (3a)–(3c) can make the multiagent system (1a)–(2) achieve structure-free containment control, if conditions in Theorem 1 (i.e., k_1, k_2, k_3 are large enough), (28), and (34a)–(34e) are satisfied.

Proof. The following Lyapunov function is constructed:

$$\begin{aligned}V_i &= \frac{1}{2}\Bigg(\underbrace{r_i^{\mathrm{T}} r_i}_{V_{1,i}} + \underbrace{E_i^{\mathrm{T}} P E_i}_{V_{2,i}} + \underbrace{\sum_{k=0}^{2} \frac{(\hat{\vartheta}_{k,i} - \bar{\vartheta}_{k,i})^2}{\bar{b}_{k,i}}}_{V_{3,i}} + \underbrace{\frac{\pi_i^2}{k_{5,i}}}_{V_{4,i}}\Bigg) \\ &= \frac{1}{2}(V_{1,i} + V_{2,i} + V_{3,i} + V_{4,i}),\end{aligned} \tag{35}$$

and the next two cases will be discussed.

Case 1. $\|r_i\| \geqslant r^{(0)}$. From (17), (18a)–(18b), (19), (24), and (33a), we have

$$\begin{aligned}\frac{1}{2}\dot{V}_{1,i} =& r_i^{\mathrm{T}}\dot{r}_i = r_i\left(-\Lambda r_i - \breve{\tau}_i + \bar{\Phi}_i - (d_i\hat{d}_i^{-1} - I_m)\breve{\tau}_i\right) \\ \leqslant& -r_i^{\mathrm{T}}\Lambda r_i - r_i^{\mathrm{T}} u_i \frac{r_i}{\|r_i\|} + \big\|r_i^{\mathrm{T}}\big\| \big\|\bar{\Phi}_i\big\| - r_i^{\mathrm{T}}(d_i\hat{d}_i^{-1} - I_m)u_i\frac{r_i}{\|r_i\|} \\ \leqslant& -r_i^{\mathrm{T}}\Lambda r_i - u_i\|r_i\| + \sum_{k=0}^{2}(\vartheta_{k,i}^* \|\bar{e}_i\|^k \|r_i\|) + \Big\|d_i\hat{d}_i^{-1} - I_m\Big\| u_i \|r_i\| \\ \leqslant& -r_i^{\mathrm{T}}\Lambda r_i + \sum_{k=0}^{2}(\vartheta_{k,i}^* \|\bar{e}_i\|^k \|r_i\|) - u_i\|r_i\| + H_i u_i \|r_i\|\end{aligned}$$

$$
\begin{aligned}
=&-r_i^{\mathrm{T}}\Lambda r_i+\sum_{k=0}^{2}(\vartheta_{k,i}^{*}\left\|\bar{e}_i\right\|^k\left\|r_i\right\|)-(1-H_i)\frac{1}{1-H_i}\sum_{k=0}^{2}(\hat{\vartheta}_{k,i}\left\|\bar{e}_i\right\|^k+\pi_i)\left\|r_i\right\|\\
\leqslant&-r_i^{\mathrm{T}}\Lambda r_i+\sum_{k=0}^{2}(\bar{\vartheta}_{k,i}\left\|\bar{e}_i\right\|^k\left\|r_i\right\|)-\sum_{k=0}^{2}(\hat{\vartheta}_{k,i}\left\|\bar{e}_i\right\|^k+\pi_i)\left\|r_i\right\|.
\end{aligned}\tag{36}
$$

From (18b), (30)–(31), and (33a), we have

$$
\begin{aligned}
\dot{V}_{2,i}=&\dot{E}_i^{\mathrm{T}}PE_i+E_i^{\mathrm{T}}P\dot{E}_i\\
=&(AE_i+B(g_i\breve{\tau}_i+\varphi_{2_i}))^{\mathrm{T}}PE_i+E_i^{\mathrm{T}}P(AE_i+B(g_i\breve{\tau}_i+\varphi_{2_i}))\\
=&E_i^{\mathrm{T}}A^{\mathrm{T}}PE_i+(B(g_i\breve{\tau}_i+\varphi_{2_i}))^{\mathrm{T}}PE_i+E_i^{\mathrm{T}}PAE_i+E_i^{\mathrm{T}}PB(g_i\breve{\tau}_i+\varphi_{2_i})\\
=&E_i^{\mathrm{T}}(A^{\mathrm{T}}P+PA)E_i+(B(g_i\breve{\tau}_i+\varphi_{2_i}))^{\mathrm{T}}PE_i+E_i^{\mathrm{T}}PB(g_i\breve{\tau}_i+\varphi_{2_i})\\
=&-E_i^{\mathrm{T}}QE_i+2E_i^{\mathrm{T}}PB(g_i\breve{\tau}_i+\varphi_{2_i})\\
=&-E_i^{\mathrm{T}}QE_i+2E_i^{\mathrm{T}}PB\left(g_iu_i\frac{r_i}{\left\|r_i\right\|}+\varphi_{2_i}\right)\\
\leqslant&-E_i^{\mathrm{T}}QE_i+2\left\|E_i^{\mathrm{T}}\right\|\left\|\varphi_{2_i}\right\|\left\|PB\right\|+2\left\|E_i^{\mathrm{T}}\right\|\left\|PBg_i\right\|u_i\frac{\left\|r_i\right\|}{\left\|r_i\right\|}\\
\leqslant&-E_i^{\mathrm{T}}QE_i+2\sum_{k=0}^{2}\bar{\vartheta}_{k,i}\left\|\bar{e}_i\right\|^k\left\|E_i\right\|+\frac{2\bar{P}_i}{1-H_i}\sum_{k=0}^{2}(\hat{\vartheta}_{k,i}\left\|\bar{e}_i\right\|^k+\pi_i)\left\|E_i\right\|.
\end{aligned}\tag{37}
$$

From (33b), we have

$$
\begin{aligned}
\dot{V}_{3,i}=&\sum_{k=0}^{2}\left\{\frac{2}{\bar{b}_{k,i}}(\hat{\vartheta}_{k,i}-\bar{\vartheta}_{k,i})(\dot{\hat{\vartheta}}_{k,i}-\dot{\bar{\vartheta}}_{k,i})\right\}\\
=&\sum_{k=0}^{2}\left\{\frac{2}{\bar{b}_{k,i}}(\hat{\vartheta}_{k,i}-\bar{\vartheta}_{k,i})\dot{\hat{\vartheta}}_{k,i}\right\}\\
=&\sum_{k=0}^{2}\left\{\frac{2}{\bar{b}_{k,i}}(\hat{\vartheta}_{k,i}-\bar{\vartheta}_{k,i})\Big(\bar{b}_{k,i}(\left\|r_i\right\|+\left\|E_i\right\|)\left\|\bar{e}_i\right\|^k\right.\\
&\left.-\bar{c}_{k,i}\hat{\vartheta}_{k,i}k_{4,i}\left\|E_i\right\|\left\|\bar{e}_i\right\|^k\Big)\right\}\\
=&2\sum_{k=0}^{2}\left\{\hat{\vartheta}_{k,i}(\left\|r_i\right\|+\left\|E_i\right\|)\left\|\bar{e}_i\right\|^k-\bar{\vartheta}_{k,i}(\left\|r_i\right\|+\left\|E_i\right\|)\left\|\bar{e}_i\right\|^k\right.\\
&\left.+\underbrace{\frac{\bar{c}_{k,i}}{\bar{b}_{k,i}}k_{4,i}}_{\bar{d}_{k,i}}\hat{\vartheta}_{k,i}\bar{\vartheta}_{k,i}\left\|E_i\right\|\left\|\bar{e}_i\right\|^k-\underbrace{\frac{\bar{c}_{k,i}}{\bar{b}_{k,i}}k_{4,i}}_{\bar{d}_{k,i}}\hat{\vartheta}_{k,i}^2\left\|E_i\right\|\left\|\bar{e}_i\right\|^k\right\}.
\end{aligned}\tag{38}
$$

From (33c), we have

$$
\begin{aligned}
\dot{V}_{4,i}=&\frac{2\pi_i\dot{\pi}_i}{k_{5,i}}\\
=&\frac{2\pi_i}{k_{5,i}}\Big\{-\pi_i\big[k_{5,i}+k_{6,i}(\left\|\bar{e}_i\right\|^5-\left\|\bar{e}_i\right\|^4)+k_{7,i}(\left\|E_i\right\|+\left\|\bar{e}_i\right\|)\big]+k_{5,i}(\left\|r_i\right\|+\left\|E_i\right\|+k_{8,i})\Big\}\\
=&2\pi_i(\left\|r_i\right\|+\left\|E_i\right\|+k_{8,i})-2\pi_i^2\left[\underbrace{\frac{k_{6,i}}{k_{5,i}}}_{k_{65,i}}(\left\|\bar{e}_i\right\|^5-\left\|\bar{e}_i\right\|^4)+\underbrace{\frac{k_{7,i}}{k_{5,i}}}_{k_{75,i}}(\left\|E_i\right\|+\left\|\bar{e}_i\right\|)+1\right].
\end{aligned}\tag{39}
$$

From (38) and (39), we have

$$\begin{aligned}\frac{1}{2}(\dot{V}_{3,i}+\dot{V}_{4,i}) =& \sum_{k=0}^{2}\Big\{\hat{\vartheta}_{k,i}(\|r_i\|+\|E_i\|)\,\|\bar{e}_i\|^k-\bar{\vartheta}_{k,i}(\|r_i\|+\|E_i\|)\,\|\bar{e}_i\|^k\\ &+\bar{d}_{k,i}\hat{\vartheta}_{k,i}\bar{\vartheta}_{k,i}\,\|E_i\|\,\|\bar{e}_i\|^k-\bar{d}_{k,i}\hat{\vartheta}_{k,i}^2\,\|E_i\|\,\|\bar{e}_i\|^k\Big\}\\ &+\pi_i(\|r_i\|+\|E_i\|+k_{8,i})-\pi_i^2[1+k_{65,i}(\|\bar{e}_i\|^5-\|\bar{e}_i\|^4)\\ &+k_{75,i}(\|E_i\|+\|\bar{e}_i\|)].\end{aligned}\tag{40}$$

By (36), (37), and (40), we can obtain

$$\begin{aligned}\dot{V}_i \leqslant& -\underbrace{\min\left\{\lambda_{\min}(\Lambda),\frac{1}{2}\lambda_{\min}(Q)\right\}}_{\chi_{\min}}(\|r_i\|^2+\|E_i\|^2)+k_{8,i}\pi_i\\ &+\underbrace{\left(1+\frac{\bar{P}_i}{1-H_i}\right)}_{\chi_i}\pi_i\,\|E_i\|-\pi_i^2[1+k_{65,i}(\|\bar{e}_i\|^5-\|\bar{e}_i\|^4)\\ &+k_{75,i}(\|E_i\|+\|\bar{e}_i\|)]+\sum_{k=0}^{2}\Bigg\{\Bigg[\left(1+\frac{\bar{P}_i}{1-H_i}\right)\hat{\vartheta}_{k,i}\\ &-\bar{d}_{k,i}\hat{\vartheta}_{k,i}^2+\bar{d}_{k,i}\hat{\vartheta}_{k,i}\bar{\vartheta}_{k,i}\Bigg]\|\bar{e}_i\|^k\,\|E_i\|\Bigg\}.\end{aligned}\tag{41}$$

For (33c), if Eqs. (34c)–(34d) hold, then $\{k_{5,i}+k_{6,i}(\|\bar{e}_i\|^5-\|\bar{e}_i\|^4)+k_{7,i}(\|E_i\|+\|\bar{e}_i\|)\}>0$, which implies that Eq. (33c) is a first-order time-varying linear system with a negative system matrix and a positive input and so does (33b) obviously, indicating that $\hat{\vartheta}_{k,i}(t)\geqslant 0$ and $\pi_i(t)\geqslant\underline{\pi_i}>0$ when $t\geqslant 0$. Note that $\|\bar{e}_i\|\geqslant\|E_i\|$, so Eq. (35) can be scaled as follows:

$$V_i\leqslant\underbrace{\max\{1,\|P\|\}}_{\chi_{\max}}(\|r_i\|^2+\|E_i\|^2)+\sum_{k=0}^{2}\frac{(\hat{\vartheta}_{k,i}^2+\bar{\vartheta}_{k,i}^2)}{\bar{b}_{k,i}}+\frac{\pi_i^2}{k_{5,i}}.\tag{42}$$

From (41) and (42), there exists the following relationship:

$$\begin{aligned}\dot{V}_i \leqslant& -\underbrace{\frac{\chi_{\min}}{\chi_{\max}}}_{\tilde{\chi}}V_i+\sum_{k=0}^{2}\frac{\tilde{\chi}(\hat{\vartheta}_{k,i}^2+\bar{\vartheta}_{k,i}^2)}{\bar{b}_{k,i}}+\frac{\tilde{\chi}\pi_i^2}{k_{5,i}}+\chi_i\pi_i\,\|E_i\|\\ &+\sum_{k=0}^{2}\Big\{(\chi_i\hat{\vartheta}_{k,i}-\bar{d}_{k,i}\hat{\vartheta}_{k,i}^2+\bar{d}_{k,i}\hat{\vartheta}_{k,i}\bar{\vartheta}_{k,i})\,\|\bar{e}_i\|^k\,\|E_i\|\Big\}\\ &+k_{8,i}\pi_i-\pi_i^2[1+k_{65,i}(\|\bar{e}_i\|^5-\|\bar{e}_i\|^4)+k_{75,i}\,\|E_i\|].\end{aligned}\tag{43}$$

Note that $\bar{d}_{k,i}$, $k_{75,i}$ are positive constants, and thus they can be split as

$$\bar{d}_{k,i}=\sum_{j=1}^{3}\bar{d}_{k,i}^{(j)},\ \ k_{75,i}=\sum_{j=1}^{2}k_{75,i}^{(j)},\tag{44}$$

where $\bar{d}_{k,i}^{(j)},k_{75,i}^{(j)}$ are positive constants. With the above decomposition, we can make the following simplification:

$$\begin{aligned}&-\bar{d}_{k,i}\hat{\vartheta}_{k,i}^2+\chi_i\hat{\vartheta}_{k,i}+\bar{d}_{k,i}\hat{\vartheta}_{k,i}\bar{\vartheta}_{k,i}\\ &=-\bar{d}_{k,i}^{(1)}\hat{\vartheta}_{k,i}^2-\bar{d}_{k,i}^{(2)}\left[\left(\hat{\vartheta}_{k,i}-\frac{\chi_i}{2\bar{d}_{k,i}^{(2)}}\right)^2-\left(\frac{\chi_i}{2\bar{d}_{k,i}^{(2)}}\right)^2\right]-\bar{d}_{k,i}^{(3)}\left[\left(\hat{\vartheta}_{k,i}-\frac{\bar{d}_{k,i}\bar{\vartheta}_{k,i}}{2\bar{d}_{k,i}^{(3)}}\right)^2-\left(\frac{\bar{d}_{k,i}\bar{\vartheta}_i}{2\bar{d}_{k,i}^{(3)}}\right)^2\right]\end{aligned}$$

$$\leqslant -\bar{d}_{k,i}^{(1)}\hat{\vartheta}_{k,i}^2+\frac{\chi_i^2}{4\bar{d}_{k,i}^{(2)}}+\frac{(\bar{d}_{k,i}\bar{\vartheta}_{k,i})^2}{4\bar{d}_{k,i}^{(3)}}, \tag{45}$$

and

$$\begin{aligned}
&-\pi_i^2(1+k_{75,i}\left\|E_i\right\|)+k_{8,i}\pi_i+\chi_i\pi_i\left\|E_i\right\| \\
&\quad=-k_{75,i}^{(1)}\pi_i^2\left\|E_i\right\|-\left[\left(\pi_i-\frac{k_{8,i}}{2}\right)^2-\left(\frac{k_{8,i}}{2}\right)^2\right]-k_{75,i}^{(2)}\left\|E_i\right\|\left[\left(\pi_i-\frac{\chi_i}{2k_{75,i}^{(2)}}\right)^2-\left(\frac{\chi_i}{2k_{75,i}^{(2)}}\right)^2\right] \\
&\quad\leqslant -k_{75,i}^{(1)}\pi_i^2\left\|E_i\right\|+\frac{k_{8,i}^2}{4}+\frac{\chi_i^2}{4k_{75,i}^{(2)}}\left\|E_i\right\|.
\end{aligned} \tag{46}$$

Since $\hat{\vartheta}_{k,i}(t)\geqslant 0$ and $\pi_i(t)\geqslant \underline{\pi_i}>0$ when $t\geqslant 0$, noting that $\left\|\bar{e}_i\right\|\geqslant\left\|E_i\right\|$, from (43), (45) and (46), we obtain

$$\begin{aligned}
\dot{V}_i\leqslant&-\tilde{\chi}V_i+\sum_{k=0}^{2}\frac{\tilde{\chi}(\hat{\vartheta}_{k,i}^2+\bar{\vartheta}_{k,i}^2)}{\bar{b}_{k,i}}+\frac{\tilde{\chi}\pi_i^2}{k_{5,i}}-\pi_i^2[k_{65,i}(\left\|\bar{e}_i\right\|^5-\left\|\bar{e}_i\right\|^4)]+\frac{\chi_i^2}{4k_{75,i}^{(2)}}\left\|E_i\right\| \\
&+\sum_{k=0}^{2}\left\{\left[-\bar{d}_{k,i}^{(1)}\hat{\vartheta}_{k,i}^2+\frac{\chi_i^2}{4\bar{d}_{k,i}^{(2)}}+\frac{(\bar{d}_{k,i}\bar{\vartheta}_{k,i})^2}{4\bar{d}_{k,i}^{(3)}}\right]\left\|\bar{e}_i\right\|^k\left\|E_i\right\|\right\}-k_{75,i}^{(1)}\pi_i^2\left\|E_i\right\|+\frac{k_{8,i}^2}{4} \\
\leqslant&-\tilde{\chi}V_i+\sum_{k=0}^{2}\frac{\tilde{\chi}(\hat{\vartheta}_{k,i}^2+\bar{\vartheta}_{k,i}^2)}{\bar{b}_{k,i}}+\frac{\tilde{\chi}\pi_i^2}{k_{5,i}}-\pi_i^2[k_{65,i}(\left\|\bar{e}_i\right\|^5-\left\|\bar{e}_i\right\|^4)]-k_{75,i}^{(1)}\pi_i^2\left\|E_i\right\|+\frac{k_{8,i}^2}{4} \\
&+\sum_{k=0}^{2}\left\{\left[\frac{\chi_i^2}{4\bar{d}_{k,i}^{(2)}}+\frac{(\bar{d}_{k,i}\bar{\vartheta}_{k,i})^2}{4\bar{d}_{k,i}^{(3)}}\right]\left\|\bar{e}_i\right\|^{k+1}\right\}+\sum_{k=0}^{2}\left(-\bar{d}_{k,i}^{(1)}\hat{\vartheta}_{k,i}^2\left\|E_i\right\|^{k+1}\right)+\frac{\chi_i^2}{4k_{75,i}^{(2)}}\left\|E_i\right\| \\
=&-\hat{\vartheta}_{0,i}^2\left(\bar{d}_{0,i}^{(1)}\left\|E_i\right\|-\frac{\tilde{\chi}}{\bar{b}_{0,i}}\right)-\hat{\vartheta}_{1,i}^2\left(\bar{d}_{1,i}^{(1)}\left\|E_i\right\|^2-\frac{\tilde{\chi}}{\bar{b}_{1,i}}\right) \\
&-\hat{\vartheta}_{2,i}^2\left(\bar{d}_{2,i}^{(1)}\left\|E_i\right\|^3-\frac{\tilde{\chi}}{\bar{b}_{2,i}}\right)-\pi_i^2\left(k_{75,i}^{(1)}\left\|E_i\right\|-\frac{\tilde{\chi}}{k_{5,i}}\right)-\tilde{\chi}V_i \\
&+\underbrace{\epsilon_5\left\|\bar{e}_i\right\|^5+\epsilon_4\left\|\bar{e}_i\right\|^4+\epsilon_3\left\|\bar{e}_i\right\|^3+\epsilon_2\left\|\bar{e}_i\right\|^2+\epsilon_1\left\|\bar{e}_i\right\|+\epsilon_0}_{f_i(\left\|\bar{e}_i\right\|)},
\end{aligned} \tag{47}$$

with

$$\epsilon_5\triangleq-\underline{\pi_i}^2k_{65,i}, \tag{48a}$$

$$\epsilon_4\triangleq\underline{\pi_i}^2k_{65,i}, \tag{48b}$$

$$\epsilon_3\triangleq\frac{\chi_i^2}{4\bar{d}_{2,i}^{(2)}}+\frac{(\bar{d}_{2,i}\bar{\vartheta}_{2,i})^2}{4\bar{d}_{2,i}^{(3)}}, \tag{48c}$$

$$\epsilon_2\triangleq\frac{\chi_i^2}{4\bar{d}_{1,i}^{(2)}}+\frac{(\bar{d}_{1,i}\bar{\vartheta}_{1,i})^2}{4\bar{d}_{1,i}^{(3)}}, \tag{48d}$$

$$\epsilon_1\triangleq\frac{\chi_i^2}{4k_{75,i}^{(2)}}+\frac{(\bar{d}_{0,i}\bar{\vartheta}_{0,i})^2}{4\bar{d}_{0,i}^{(3)}}+\frac{\chi_i^2}{4\bar{d}_{3,i}^{(2)}}, \tag{48e}$$

$$\epsilon_0\triangleq\frac{k_{8,i}^2}{4}+\sum_{k=0}^{2}\frac{\tilde{\chi}\bar{\vartheta}_{k,i}^2}{\bar{b}_{k,i}}. \tag{48f}$$

According to Descartes' rule of sign change and Bolzano's Theorem, we can infer that $f_i(\left\|\bar{e}_i\right\|)$ has only one positive real root, here, defined as $\rho_i\in\mathbb{R}^+$. Notice that $\epsilon_5<0$, resulting in $f_i(\left\|\bar{e}_i\right\|)\leqslant 0$ when $\left\|\bar{e}_i\right\|\geqslant\rho_i$. Thus, from (47), $\dot{V}_i\leqslant-\tilde{\chi}V_i$ can be guaranteed if

$$\left\|\bar{e}_i\right\|\geqslant\rho_i,\ \left\|E_i\right\|\geqslant\max\{\rho_{0_i},\rho_{1_i},\rho_{2_i},\rho_{3_i}\}, \tag{49}$$

where $\rho_{0_i} \triangleq \frac{\tilde{\chi}}{\bar{b}_{0,i}\bar{d}_{0,i}^{(1)}}$, $\rho_{1_i} \triangleq \sqrt{\frac{\tilde{\chi}}{\bar{b}_{1,i}\bar{d}_{1,i}^{(1)}}}$, $\rho_{2_i} \triangleq \sqrt[3]{\frac{\tilde{\chi}}{\bar{b}_{2,i}\bar{d}_{2,i}^{(1)}}}$, $\rho_{3_i} \triangleq \frac{\tilde{\chi}}{k_{5,i}k_{75,i}^{(1)}}$.

Notice that $\|E_i\| \leqslant \|\bar{e}_i\|$; thus Eq. (49) is equivalent to

$$\|E_i\| \geqslant \max\{\rho_i, \rho_{0_i}, \rho_{1_i}, \rho_{2_i}, \rho_{3_i}\}. \tag{50}$$

Case 2. $\|r_i\| < r^{(0)}$. The proof steps are the same as those in Case 1, but the corresponding differences are reflected in the following formulas.

(i) Eq. (36) in Case 1 corresponds to

$$\begin{aligned}\frac{1}{2}\dot{V}_{1,i} =& r_i\left(-\Lambda r_i - u_i\frac{r_i}{r^{(0)}} + \bar{\Phi}_i - (d_i\hat{d}_i^{-1} - I_m)u_i\frac{r_i}{r^{(0)}}\right)\\ \leqslant& -r_i^{\mathrm{T}}\Lambda r_i - u_i\frac{\|r_i\|^2}{r^{(0)}} + r_i^{\mathrm{T}}\bar{\Phi}_i - (d_i\hat{d}_i^{-1} - I_m)u_i\frac{\|r_i\|^2}{r^{(0)}}\\ \leqslant& -r_i^{\mathrm{T}}\Lambda r_i + \sum_{k=0}^{2}(\bar{\vartheta}_{k,i}\|\bar{e}_i\|^k\|r_i\|) - \sum_{k=0}^{2}\left[(\hat{\vartheta}_{k,i}\|\bar{e}_i\|^k + \pi_i)\frac{\|r_i\|^2}{r^{(0)}}\right].\end{aligned} \tag{51}$$

(ii) From (37)–(40) and (51), Eq. (41) in Case 1 corresponds to

$$\begin{aligned}\dot{V}_i \leqslant& -\underbrace{\min\left\{\lambda_{\min}(\Lambda), \frac{1}{2}\lambda_{\min}(Q)\right\}}_{\chi_{\min}}(\|r_i\|^2 + \|E_i\|^2) + k_{8,i}\pi_i\\ &- \pi_i^2\left[1 + k_{65,i}(\|\bar{e}_i\|^5 - \|\bar{e}_i\|^4) + k_{75,i}\|E_i\|\right]\\ &+ \sum_{k=0}^{2}\left[(\chi_i\hat{\vartheta}_{k,i} - \bar{d}_{k,i}\hat{\vartheta}_{k,i}^2 + \bar{d}_{k,i}\hat{\vartheta}_{k,i}\bar{\vartheta}_{k,i})\|\bar{e}_i\|^k\|E_i\|\right]\\ &+ \sum_{k=0}^{2}(\hat{\vartheta}_{k,i}\|\bar{e}_i\|^k\|r_i\|) - \pi_i^2 k_{75,i}\|\bar{e}_i\| + \pi_i\|r_i\|\\ &- \sum_{k=0}^{2}\left[\hat{\vartheta}_{k,i}\|\bar{e}_i\|^k\frac{\|r_i\|^2}{r^{(0)}}\right] - \pi_i\frac{\|r_i\|^2}{r^{(0)}} + \chi_i\pi_i\|E_i\|.\end{aligned} \tag{52}$$

(iii) From (42) and (52), Eq. (43) in Case 1 corresponds to

$$\begin{aligned}\dot{V}_i \leqslant& -\underbrace{\frac{\chi_{\min}}{\chi_{\max}}}_{\tilde{\chi}}V_i + \sum_{k=0}^{2}\frac{\tilde{\chi}(\hat{\vartheta}_{k,i}^2 + \bar{\vartheta}_{k,i}^2)}{\bar{b}_{k,i}} + \frac{\tilde{\chi}\pi_i^2}{k_{5,i}} + \chi_i\pi_i\|E_i\|\\ &+ \sum_{k=0}^{2}\left[(\chi_i\hat{\vartheta}_{k,i} - \bar{d}_{k,i}\hat{\vartheta}_{k,i}^2 + \bar{d}_{k,i}\hat{\vartheta}_{k,i}\bar{\vartheta}_{k,i})\|\bar{e}_i\|^k\|E_i\|\right]\\ &+ k_{8,i}\pi_i - \pi_i^2\left[1 + k_{65,i}(\|\bar{e}_i\|^5 - \|\bar{e}_i\|^4) + k_{75,i}\|E_i\|\right]\\ &+ \sum_{k=0}^{2}\left(\hat{\vartheta}_{k,i}\|\bar{e}_i\|^k r^{(0)}\right) + \pi_i r^{(0)}.\end{aligned} \tag{53}$$

(iv) Note that Eq. (46) in Case 1 corresponds to

$$\begin{aligned}&-\pi_i^2(1 + k_{75,i}\|E_i\|) + \pi_i(k_{8,i} + r^{(0)}) + \chi_i\pi_i\|E_i\|\\ &= -k_{75,i}^{(1)}\pi_i^2\|E_i\| - \left[\left(\pi_i - \frac{k_{8,i} + r^{(0)}}{2}\right)^2 - \left(\frac{k_{8,i} + r^{(0)}}{2}\right)^2\right]\\ &\quad - k_{75,i}^{(2)}\|E_i\|\left[\left(\pi_i - \frac{\chi_i}{2k_{75,i}^2}\right)^2 - \left(\frac{\chi_i}{2k_{75,i}^2}\right)^2\right]\end{aligned}$$

$$\leqslant -k_{75,i}^{(1)}\pi_i^2\left\|E_i\right\| + \frac{\chi_i^2}{4k_{75,i}^2}\left\|E_i\right\| + \frac{(k_{8,i}+r^{(0)})^2}{4}, \tag{54}$$

and the basic inequality

$$\sum_{k=0}^{2}\left(\hat{\vartheta}_{k,i}^2 + \left\|\bar{e}_i\right\|^{2k}\frac{{r^{(0)}}^2}{4}\right) \geqslant \sum_{k=0}^{2} r^{(0)}\hat{\vartheta}_{k,i}\left\|\bar{e}_i\right\|^k. \tag{55}$$

(v) By (45), (53)–(55), Eqs. (47), (48a)–(48f), and (50) in Case 1 correspond to

$$\begin{aligned}
\dot{V}_i \leqslant & -\tilde{\chi}V_i + \sum_{k=0}^{2}\frac{\tilde{\chi}(\hat{\vartheta}_{k,i}^2+\bar{\vartheta}_{k,i}^2)}{\bar{b}_{k,i}} + \frac{\tilde{\chi}\pi_i^2}{k_{5,i}} + \frac{(k_{8,i}+r^{(0)})^2}{4} \\
& + \sum_{k=0}^{2}\left\{\left[\frac{\chi_i^2}{4\bar{d}_{k,i}^{(2)}} + \frac{(\bar{d}_{k,i}\bar{\vartheta}_{k,i})^2}{4\bar{d}_{k,i}^{(3)}}\right]\left\|\bar{e}_i\right\|^{k+1}\right\} + \pi_i^2 \\
& - \underline{\pi_i}^2 k_{65,i}(\left\|\bar{e}_i\right\|^5 - \left\|\bar{e}_i\right\|^4) - k_{75,i}^{(1)}\pi_i^2\left\|E_i\right\| + \frac{\chi_i^2}{4k_{75,i}^{(2)}}\left\|E_i\right\| \\
& + \sum_{k=0}^{2}\left(\hat{\vartheta}_{k,i}^2 + \left\|\bar{e}_i\right\|^{2k}\frac{{r^{(0)}}^2}{4}\right) - \sum_{k=0}^{2}\left(\bar{d}_{k,i}^{(1)}\hat{\vartheta}_{k,i}^2\left\|E_i\right\|^{k+1}\right) \\
= & -\tilde{\chi}V_i - \hat{\vartheta}_{0,i}^2\left[\bar{d}_{0,i}^{(1)}\left\|E_i\right\| - \left(\frac{\tilde{\chi}}{\bar{b}_{0,i}}+1\right)\right] - \hat{\vartheta}_{1,i}^2\left[\bar{d}_{1,i}^{(1)}\left\|E_i\right\|^2 - \left(\frac{\tilde{\chi}}{\bar{b}_{1,i}}+1\right)\right] \\
& - \hat{\vartheta}_{2,i}^2\left[\bar{d}_{2,i}^{(1)}\left\|E_i\right\|^3 - \left(\frac{\tilde{\chi}}{\bar{b}_{2,i}}+1\right)\right] - \pi_i^2\left[k_{75,i}^{(1)}\left\|E_i\right\| - \left(\frac{\tilde{\chi}}{k_{5,i}}+1\right)\right] \\
& + \underbrace{\acute{\epsilon}_5\left\|\bar{e}_i\right\|^5 + \acute{\epsilon}_4\left\|\bar{e}_i\right\|^4 + \acute{\epsilon}_3\left\|\bar{e}_i\right\|^3 + \acute{\epsilon}_2\left\|\bar{e}_i\right\|^2 + \acute{\epsilon}_1\left\|\bar{e}_i\right\| + \acute{\epsilon}_0}_{\acute{f}_i(\left\|\bar{e}_i\right\|)},
\end{aligned} \tag{56}$$

with

$$\acute{\epsilon}_5 \triangleq -\underline{\pi_i}^2 k_{65,i}, \tag{57a}$$

$$\acute{\epsilon}_4 \triangleq \underline{\pi_i}^2 k_{65,i} + \frac{(r^{(0)})^2}{4}, \tag{57b}$$

$$\acute{\epsilon}_3 \triangleq \frac{\chi_i^2}{4\bar{d}_{2,i}^{(2)}} + \frac{(\bar{d}_{2,i}\bar{\vartheta}_{2,i})^2}{4\bar{d}_{2,i}^{(3)}}, \tag{57c}$$

$$\acute{\epsilon}_2 \triangleq \frac{\chi_i^2}{4\bar{d}_{1,i}^{(2)}} + \frac{(\bar{d}_{1,i}\bar{\vartheta}_{1,i})^2}{4\bar{d}_{1,i}^{(3)}} + \frac{(r^{(0)})^2}{4}, \tag{57d}$$

$$\acute{\epsilon}_1 \triangleq \frac{\chi_i^2}{4\bar{d}_{0,i}^{(2)}} + \frac{(\bar{d}_{0,i}\bar{\vartheta}_{0,i})^2}{4\bar{d}_{0,i}^{(3)}} + \frac{\chi_i^2}{4k_{75,i}^{(2)}}, \tag{57e}$$

$$\acute{\epsilon}_0 \triangleq \sum_{k=0}^{2}\frac{\tilde{\chi}\bar{\vartheta}_{k,i}^2}{\bar{b}_{k,i}} + \frac{(r^{(0)})^2}{4} + \frac{(k_{8,i}+r^{(0)})^2}{4}. \tag{57f}$$

Similar to the analysis in Case 1, $\dot{V}_i \leqslant -\tilde{\chi}V_i$ can be guaranteed if

$$\left\|E_i\right\| \geqslant \max\{\acute{\rho}_i, \acute{\rho}_{0_i}, \acute{\rho}_{1_i}, \acute{\rho}_{2_i}, \acute{\rho}_{3_i}\}, \tag{58}$$

where $\acute{\rho}_{0_i} \triangleq (\frac{\tilde{\chi}}{\bar{b}_{0,i}}+1)/\bar{d}_{0,i}^{(1)}$, $\acute{\rho}_{1_i} \triangleq \sqrt{(\frac{\tilde{\chi}}{\bar{b}_{1,i}}+1)/\bar{d}_{1,i}^{(1)}}$, $\acute{\rho}_{2_i} \triangleq \sqrt[3]{(\frac{\tilde{\chi}}{\bar{b}_{2,i}}+1)/\bar{d}_{2,i}^{(1)}}$, and $\acute{\rho}_{3_i} \triangleq (\frac{\tilde{\chi}}{k_{5,i}}+1)/k_{75,i}^{(1)}$. $\acute{\rho}_i \in \mathbb{R}^+$ is the only positive real root of $\acute{f}_i(\left\|\bar{e}_i\right\|)$.

Combining the above two cases can yield uniformly ultimately bounded (UUB) stability, which means $e_{i_u}, \dot{e}_{i_u}, r_i, \hat{\vartheta}_{k,i}, \pi_i \in \mathcal{L}_\infty$. Note that Eq. (16c) can be rewritten as

$$\dot{e}_{i_a} = K_a^{-1}r_i - K_a^{-1}\Theta_a e_{i_a} - K_a^{-1}K_u\dot{e}_{i_u} - K_a^{-1}\Theta_u e_{i_u}. \tag{59}$$

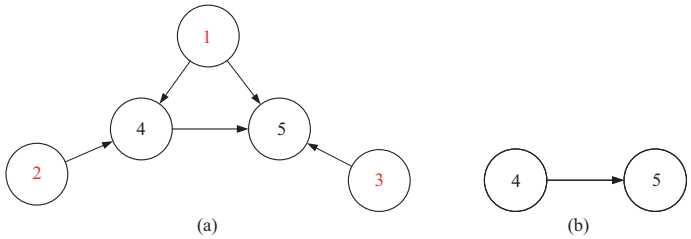

Figure 1 (Color online) Communication topology for the graph $\bar{\mathcal{G}}_{\mathcal{A}}$ and the subgraph $\mathcal{G}_A$. (a) The leaders and followers (nodes 1–3 are leaders and 4 and 5 are followers); (b) The followers.

By selecting $K_a, \Theta_a \in \mathbb{R}^{m\times m} > 0$ satisfying $K_a^{-1}\Theta_a > 0$, with the conclusion that $e_{i_u}, \dot{e}_{i_u}, r_i, \hat{\vartheta}_{k,i}, \pi_i \in \mathcal{L}_\infty$, we can draw a conclusion that $e_{i_a}, \dot{e}_{i_a} \in \mathcal{L}_\infty$, which is proven that each follower in the following layer converges to a small neighborhood around the corresponding virtual node in the virtual layer. Note that the virtual layer can converge to the convex hull $\mathrm{Co}(\mathcal{Q}_{\mathcal{R}})$ according to Theorem 1, the final conclusion is that each follower in the following layer converges to the convex hull $\mathrm{Co}(\mathcal{Q}_{\mathcal{R}})$ formed by N_r leaders.

Remark 6. The problem discussed in this paper is the structure-free containment control for uncertain underactuated MELSs considering disturbances. To achieve this, a layered approach is applied. Compared with the earlier research studies [6, 11–15, 18, 19, 22, 23], the methods in this paper have some advantages and breakthroughs. In [11–15], specific physical constraints or the structural symmetry condition of the mass matrix were necessary in the process of control, which severely limited the range of underactuated EL systems that could be controlled. Besides, Refs. [18, 19, 22, 23] ignored external disturbances and system uncertainties during control, which are well known to exist in practical applications everywhere. This resulted in poor robustness. In contrast, it is more practical to consider full-dimensional external disturbances and system uncertainties in this paper. Furthermore, notice that Refs. [6, 22, 23] were based on general linear systems or full-actuated EL systems, but in practice, underactuated EL systems are more widely used with the advantages of lightweight, low energy consumption, and excellent performance, making it meaningful to do more discussion and research on this type of more complex nonlinear system.

5 Simulation examples

Through the following simulation, we are going to verify our theoretical results. The network $\bar{\mathcal{G}}_{\mathcal{A}}$ shown in Figure 1(a) consists of three leaders (i.e., nodes 1–3) and two followers (i.e., nodes 4 and 5). The Laplacian matrix is given as follows:

$$\mathcal{L} = \begin{bmatrix} 0 & 0 & 0 & 0 & 0 \\ 0 & 0 & 0 & 0 & 0 \\ 0 & 0 & 0 & 0 & 0 \\ -1 & -1 & 0 & 3 & -1 \\ -1 & 0 & -1 & -1 & 3 \end{bmatrix}.$$

It is obvious that the subgraph $\mathcal{G}_{\mathcal{A}}$ shown in Figure 1(b) is strongly connected, which is consistent with Assumption 5. And the following underactuated MELSs are simulated:

$$\begin{bmatrix} M_{i_{11}}, M_{i_{12}}, M_{i_{13}} \\ M_{i_{21}}, M_{i_{22}}, M_{i_{23}} \\ M_{i_{31}}, M_{i_{32}}, M_{i_{33}} \end{bmatrix} \begin{bmatrix} \ddot{q}_{i_1} \\ \ddot{q}_{i_2} \\ \ddot{q}_{i_3} \end{bmatrix} + \begin{bmatrix} V_{m_{i_{11}}}, V_{m_{i_{12}}}, V_{m_{i_{13}}} \\ V_{m_{i_{21}}}, V_{m_{i_{22}}}, V_{m_{i_{23}}} \\ V_{m_{i_{31}}}, V_{m_{i_{32}}}, V_{m_{i_{33}}} \end{bmatrix} \begin{bmatrix} \dot{q}_{i_1} \\ \dot{q}_{i_2} \\ \dot{q}_{i_3} \end{bmatrix} + \begin{bmatrix} G_{i_1} \\ G_{i_2} \\ G_{i_3} \end{bmatrix} + \begin{bmatrix} \varpi_{i_1} \\ \varpi_{i_2} \\ \varpi_{i_3} \end{bmatrix} = \begin{bmatrix} \tau_{i_1} \\ \tau_{i_2} \\ 0 \end{bmatrix}, \ i = 4, 5,$$

where $q_i = [q_{i_1}\ q_{i_2}\ q_{i_3}]^{\mathrm{T}}$. $M_{i_{11}} = J_z + m_0 P_z^2$, $M_{i_{12}} = -m_0 P_z \cos(q_{i_1} - q_{i_3})$, $M_{i_{13}} = -m_0 P_z q_{i_2} \sin(q_{i_1} - q_{i_3})$, $M_{i_{21}} = -m_0 P_z \cos(q_{i_1} - q_{i_3})$, $M_{i_{22}} = m_0$, $M_{i_{23}} = 0$, $M_{i_{31}} = -m_0 P_z q_{i_2} \sin(q_{i_1} - q_{i_3})$, $M_{i_{32}} = 0$, $M_{i_{33}} = m_0 q_{i_2}^2$. $V_{m_{i_{11}}} = 0$, $V_{m_{i_{12}}} = -m_0 P_z \sin(q_{i_1} - q_{i_3})\dot{q}_{i_3}$, $V_{m_{i_{13}}} = -m_0 P_z[\sin(q_{i_1} - q_{i_3})\dot{q}_{i_2} - \cos(q_{i_1} - q_{i_3})q_{i_2}\dot{q}_{i_3}]$, $V_{m_{i_{21}}} = m_0 P_z \sin(q_{i_1} - q_{i_3})\dot{q}_{i_1}$, $V_{m_{i_{22}}} = 0$, $V_{m_{i_{23}}} = -m_0 q_{i_2}\dot{q}_{i_3}$, $V_{m_{i_{31}}} = -m_0 P_z q_{i_2} \cos(q_{i_1} - q_{i_3})\dot{q}_{i_1}$, $V_{m_{i_{32}}} = m_0 q_{i_2}\dot{q}_{i_3}$, $V_{m_{i_{33}}} = m_0 q_{i_2}\dot{q}_{i_2}$. $G_{i_1} = (m_0 P_z + m_z d_z) g \cos(q_{i_1})$, $G_{i_2} = -m_0 g \cos(q_{i_3})$, $G_{i_3} = m_0 g q_{i_2} \sin(q_{i_3})$. $\varpi_{i_1} = \varpi_{i_2} = \varpi_{i_3} = 0.01\sin(0.01t)$. $J_z = 6.5\ \mathrm{kg}\cdot\mathrm{m}^2$, $m_0 = 0.5$ kg, $\hat{J}_z = 6\ \mathrm{kg}\cdot\mathrm{m}^2$, $\hat{m}_0 = 0.45$ kg, $P_z = 0.8$ m, $m_z = 20$ kg, $d_z = 0.4$ m, $g = 9.8\ \mathrm{m/s}^2$.

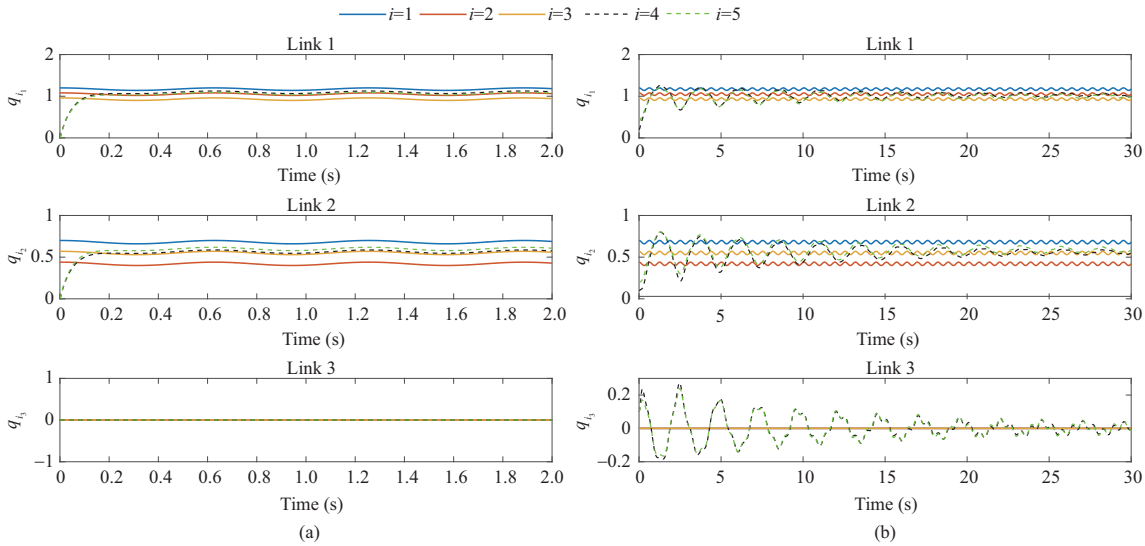

Figure 2 (Color online) (a) Containment observer (3a)–(3c) of the positions $q_i = [q_{i_1}\ q_{i_2}\ q_{i_3}]^{\mathrm{T}}, i = 1, 2, 3, 4, 5$, for three leaders and two virtual nodes. (b) Adaptive robust tracking controller (18a) and (18b) of the positions $q_i = [q_{i_1}\ q_{i_2}\ q_{i_3}]^{\mathrm{T}}, i = 1, 2, 3, 4, 5$, for three leaders and two followers.

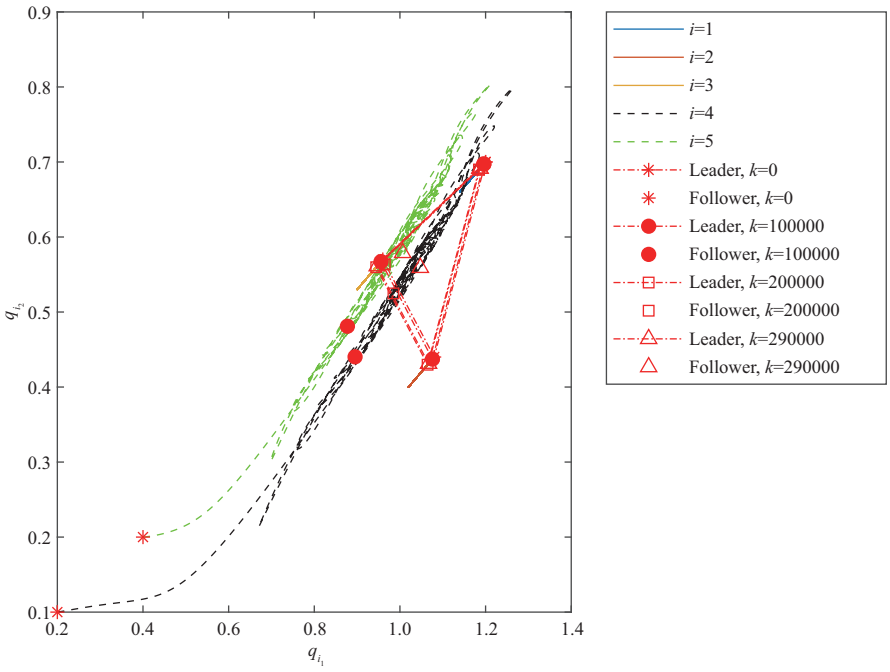

Figure 3 (Color online) Simulation results for positions of followers and leaders.

Based on Assumptions 1 and 2, three desired trajectories are chosen as

$$q_1 = [1.17 + 0.03\cos(10t);\ 0.68 + 0.02\cos(10t);\ 0],$$
$$q_2 = [1.05 + 0.03\cos(10t);\ 0.42 + 0.02\cos(10t);\ 0],$$
$$q_3 = [0.93 + 0.03\cos(10t);\ 0.55 + 0.02\cos(10t);\ 0].$$

First, $S_i, C_i, \xi_i, \dot{q}_i, i = 4, 5$ are initialized to zero and $q_4(0) = [0.2\ 0.1\ 0.1]^{\mathrm{T}}$, $q_5(0) = [0.4\ 0.2\ 0.1]^{\mathrm{T}}$.

Second, the control parameters k_1, k_2, k_3 from (3a)–(3c) are chosen as $k_1 = k_2 = 10, k_3 = 100$ to satisfy Theorem 1.

Third, set $K_a = 50I_2$, $K_u = 50[1\ 1]^{\mathrm{T}}$, $\Theta_a = 400I_2$, $\Theta_u = 400[1\ 1]^{\mathrm{T}}$, $\Lambda = 15I_2$, $r^{(0)} = 1$. According to Theorem 2, select $K = [1\ 1]^{\mathrm{T}}$ satisfying (28), $\hat{\vartheta}_{k,i}(0) = 10, k = 0, 1, 2$ satisfying (34a), $\pi_i(0) = 10$

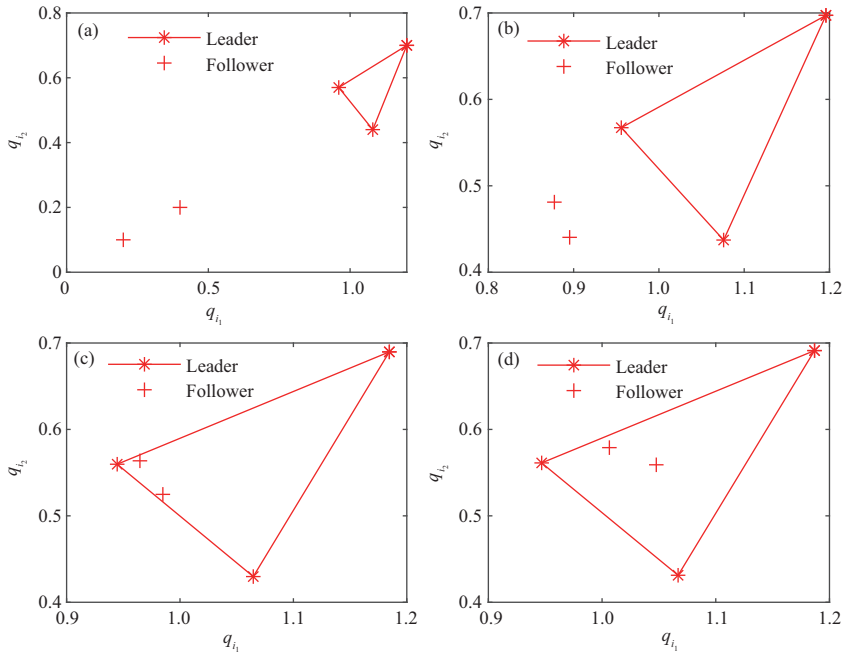

Figure 4 (Color online) Position trajectory snapshots at different iteration steps. (a) $k = 0$; (b) $k = 100000$; (c) $k = 200000$; (d) $k = 290000$.

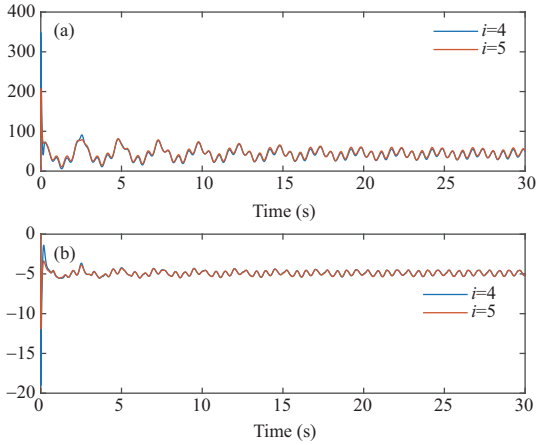

Figure 5 (Color online) Values of the control torque τ_i. (a) Link 1; (b) link 2.

satisfying (34b).

Fourth, calculate $H_i = 0.5$ according to Proposition 3. Set $Q = I_2$, thus $\bar{P}_i = 1$.

Finally, according to Theorem 2, select $\bar{b}_{0,i} = 3$, $\bar{b}_{1,i} = 4$, $\bar{b}_{2,i} = 1$, $\bar{c}_{0,i} = 1$, $\bar{c}_{1,i} = 4$, $\bar{c}_{2,i} = 1$, $k_{5,i} = 2$, $k_{6,i} = k_{7,i} = k_{8,i} = 1$ satisfying (34c)–(34d); select $k_{4,i} = 3.5, i = 4, 5$ satisfying (34e).

The positions of three leaders, two virtual nodes, and two followers are depicted in Figure 2, from which it can be observed that the convex hull can be well estimated by the designed containment observer (3a)–(3c) and UUB stability can be achieved by the proposed adaptive robust tracking controller (18a) and (18b). Figure 3 shows all the information throughout the simulation. For a clearer view, we have isolated some of the information and presented it in Figure 4. The four red triangles are the convex hulls formed by the leaders at, respectively, $t = 0$ s, $t = 10$ s, $t = 20$ s, $t = 29$ s. It is clearly shown that the two followers can converge to the convex hull formed by three leaders. The curves of the control inputs τ_i and various gains $\hat{\vartheta}_{k,i}$, π_i, u_i are plotted in Figures 5–7. From the simulation results, we can conclude that the proposed hierarchical adaptive robust containment control method can achieve structure-free containment control for uncertain underactuated MELSs with disturbances.

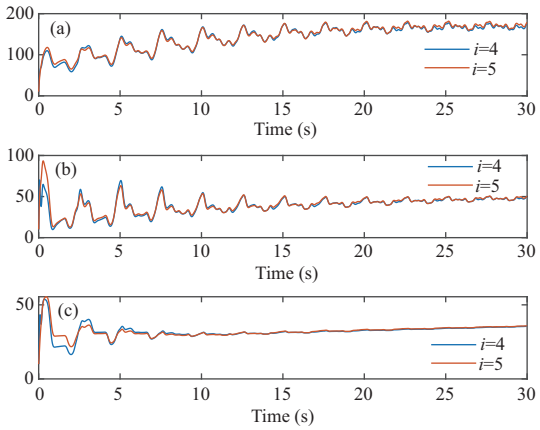

Figure 6 (Color online) Values of (a) $\hat{\vartheta}_{0,i}$, (b) $\hat{\vartheta}_{1,i}$, and (c) $\hat{\vartheta}_{2,i}$.

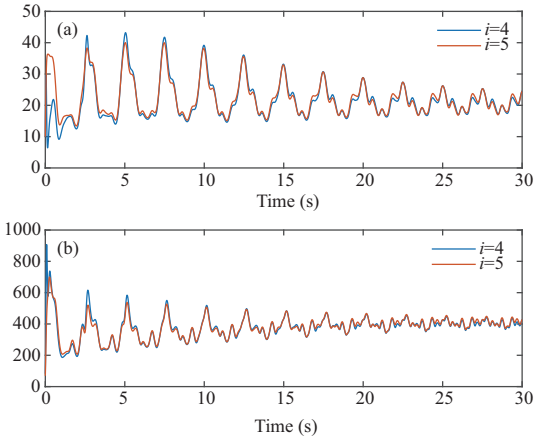

Figure 7 (Color online) Values of (a) π_i and (b) u_i.

6 Conclusion

This paper studies the problem of structure-free distributed containment control for uncertain underactuated MELSs considering disturbances by using a layered approach. First, the second layer is the virtual layer constructed artificially for hierarchical control. We move all virtual nodes to the convex hull formed by leaders in the first layer by implementing containment control algorithms on all virtual nodes. Then, the third layer is the following layer, and we propose an adaptive robust tracking controller to ensure that each follower in the third layer tracks the corresponding virtual node in the second layer. So far, the underactuated MELSs can achieve containment control. Furthermore, through the theoretical derivation, sufficient conditions are obtained to achieve the objective of structure-free containment control. Finally, the effectiveness of the proposed stratified structure-free containment control method is verified by a simulation example.

In the future, we will extend our study to the actuator saturation constraint and collision avoidance problem.

Acknowledgements This work was supported in part by National Natural Science Foundation of China (Grant Nos. 61991412, 62273159, U22A6007) and Program for HUST Academic Frontier Youth Team (Grant No. 2018QYTD07).

References

1 Ma L F, Wang Z D, Han Q-L, et al. Consensus control of stochastic multi-agent systems: a survey. Sci China Inf Sci, 2017, 60: 120201
2 Martin S, Girard A, Fazeli A, et al. Multiagent flocking under general communication rule. IEEE Trans Control Netw Syst, 2014, 1: 155–166
3 Wen G X, Chen C L P, Dou H, et al. Formation control with obstacle avoidance of second-order multi-agent systems under directed communication topology. Sci China Inf Sci, 2019, 62: 192205
4 Chen J, Gan M G, Huang J, et al. Formation control of multiple Euler-Lagrange systems via null-space-based behavioral control. Sci China Inf Sci, 2016, 59: 010202
5 Wang S, Jin X, Mao S, et al. Model-free event-triggered optimal consensus control of multiple Euler-Lagrange systems via reinforcement learning. IEEE Trans Netw Sci Eng, 2021, 8: 246–258
6 Zhao K, Song Y, Ma T, et al. Prescribed performance control of uncertain Euler-Lagrange systems subject to full-state constraints. IEEE Trans Neural Netw Learn Syst, 2018, 29: 3478–3489
7 Ashrafiuon H, Erwin R S. Sliding mode control of underactuated multibody systems and its application to shape change control. Int J Control, 2008, 81: 1849–1858
8 Olfati-Saber R. Normal forms for underactuated mechanical systems with symmetry. IEEE Trans Automat Contr, 2002, 47: 305–308
9 Lu B, Fang Y, Sun N. Modeling and nonlinear coordination control for an underactuated dual overhead crane system. Automatica, 2018, 91: 244–255
10 Liu Z, Yan Q. Controller design and simulation of underactuated pendulum. In: Proceedings of the IEEE Chinese Control and Decision Conference (CCDC), 2011. 2767–2771
11 Huang J, Ri S, Fukuda T, et al. A disturbance observer based sliding mode control for a class of underactuated robotic system with mismatched uncertainties. IEEE Trans Automat Contr, 2019, 64: 2480–2487
12 Lu B, Fang Y, Sun N. Continuous sliding mode control strategy for a class of nonlinear underactuated systems. IEEE Trans Automat Contr, 2018, 63: 3471–3478
13 Nersesov S G, Ashrafiuon H, Ghorbanian P. On estimation of the domain of attraction for sliding mode control of underactuated nonlinear systems. Int J Robust Nonlinear Control, 2014, 24: 811–824

14 Sarras I, Acosta J, Ortega R, et al. Constructive immersion and invariance stabilization for a class of underactuated mechanical systems. Automatica, 2013, 49: 1442–1448
15 Xu R, Özgüner Ü. Sliding mode control of a class of underactuated systems. Automatica, 2008, 44: 233–241
16 Yoo S J, Park B S. Guaranteed performance design for distributed bounded containment control of networked uncertain underactuated surface vessels. J Franklin Institute, 2017, 354: 1584–1602
17 Liu Z W, Hou H, Wang Y W. Formation-containment control of multiple underactuated surface vessels with sampling communication via hierarchical sliding mode approach. ISA Trans, 2019, 124: 458–467
18 Cai H, Huang J. The leader-following consensus for multiple uncertain euler-lagrange systems with an adaptive distributed observer. IEEE Trans Automat Contr, 2016, 61: 3152–3157
19 Lu M, Liu L. Leader-following consensus of multiple uncertain euler-lagrange systems with unknown dynamic leader. IEEE Trans Automat Contr, 2019, 64: 4167–4173
20 Wang L, He H, Zeng Z, et al. Model-independent formation tracking of multiple Euler-Lagrange systems via bounded inputs. IEEE Trans Cybern, 2021, 51: 2813–2823
21 Wei B, Xiao F, Fang F, et al. Velocity-free event-triggered control for multiple Euler-Lagrange systems with communication time delays. IEEE Trans Automat Contr, 2021, 66: 5599–5605
22 Hua Y, Dong X, Li Q, et al. Distributed time-varying formation robust tracking for general linear multiagent systems with parameter uncertainties and external disturbances. IEEE Trans Cybern, 2017, 47: 1959–1969
23 Li D, Zhang W, He W, et al. Two-layer distributed formation-containment control of multiple Euler-Lagrange systems by output feedback. IEEE Trans Cybern, 2019, 49: 675–687
24 Bidram A, Davoudi A, Lewis F L, et al. Distributed cooperative secondary control of microgrids using feedback linearization. IEEE Trans Power Syst, 2013, 28: 3462–3470
25 Spong M W, Hutchinson S, Vidyasagar M. Robot Dynamics and Control. Hoboken: John Wiley and Sons, 2004
26 Ren W, Cao Y. Distributed Coordination of Multi-Agent Networks: Emergent Problems, Models, and Issues. London: Springer-Verlag, 2011
27 Kim T, Lee C, Shim H. Completely decentralized design of distributed observer for linear systems. IEEE Trans Automat Contr, 2020, 65: 4664–4678
28 Su Y, Huang J. Cooperative output regulation with application to multi-agent consensus under switching network. IEEE Trans Syst Man Cybern B, 2012, 42: 864–875
29 Shtessel Y, Taleb M, Plestan F. A novel adaptive-gain supertwisting sliding mode controller: methodology and application. Automatica, 2012, 48: 759–769